A novel type of organometallic 2-R-2,4-dihydro- 1H-3,1-benzoxazine with R = [M(η5-C5H4)(CO)3] (M = Re or Mn) units. Experimental and computational studies of the effect of substituent R on ring-chain tautomerism†

Juan Oyarzo, [a] Ramón Bosque, [b] Patricia Toro, [a] Carlos P. Silva, [c] Rodrigo Arancibia, [d] Mercè Font-Bardía, [e] Vania Artigas, [a] Carme Calvis,[f] Ramon Messeguer, [f] A. Hugo Klahn *[a] and Concepción López*[b]

a Instituto de Química, Pontificia Universidad Católica de Valparaíso, Casilla 4059, Valparaíso, Chile.
b Secció de Química Inorgànica del Departament de Química Inorgànica i Orgànica, Facultat de Química, Universitat de Barcelona, Martí I Franquès 1-11, E-08028-Barcelona, Spain.
c Departamento de Química de los Materiales, Facultad de Química y Biología, Universidad de Santiago de Chile, Soft Matter Research-Technology Center, SMAT-C, Av. B. O'Higgins 3363, Casilla 40, Correo 33, Santiago, Chile
d Laboratorio de Química Inorgánica y Organometálica, Departamento de Química Analítica e Inorgánica, Facultad de Ciencias Químicas, Universidad de Concepción, Concepción, Chile
e Unitat de Difracció de Raig-X, Centres Científics i Tecnològics (CCiT), Universitat de Barcelona, Solé i Sabaris, 1-3, E-08028-Barcelona, Spain
f Biomed Division, Health & Biomedicine Unit, LEITAT Technological Center, Parc Científic de Barcelona, Edifici Hèlix, Baldiri i Reixach 13-21, E-08028-Barcelona, Spain

Hugo Klahn: Hugo.klahn@pucv.cl
Concepción López: conchi.lopez@qi.ub.es

ABSTRACT:

The syntheses, characterization, X-ray crystal structures, electrochemical properties and anticancer and antichagasic activities of the first examples of 2-substituted 2,4-dihydro-1H-3,1-benzoxazines with halfsandwich organometallic arrays, [M(η5-C5H4)(CO)3] (M = Re or Mn), at position-2 are described. Experimental and computational studies based on DFT calculations on the open forms [Schiff bases of general formulae R-CHvN-C6H4-2-CH2OH] (5), with R = ferrocenyl (a), phenyl (b), cyrhetrenyl (c) or cymantrenyl (d), and their tautomeric forms (2-substituted 2,4-dihydro-1H-3,1 benzoxazines) haveallowed us to establish the influence of substituents a–d and solvents on: (a) the extent of tautomeric equilibria (5a–5d) ↔ (6a–6d) and (b) their electrochemical properties and the electronic distribution on the open and closed forms. Despite the formal similarity between 6c and 6d, their anticancer and antiparasitic activities are markedly different. Compound 6d is inactive in the HCT116, MDA-MB231 and MCF7 cancer cell lines, but 6c shows moderate activity in the latter cell line, while the Mn(I) complex (6d) is a more potent anti-Trypanosoma cruzi agent than its Re(I) analogue (6c).

..

Introduction

Ring-chain tautomerism involving 1,3-N,E (E = S or O) heterocycles has attracted great attention for a long time.1–4 In this sort of process an iminothiol or an iminoalcohol undergo a reversible intramolecular C–H addition giving 1,3-N,E heterocycles via a 5- or a 6-endo-trig process (Scheme 1A and B).1–4 This type of tautomerism is important in synthesis, catalysis and also in physical and medicinal chemistry.1–7 For E = O, the 6-endo trig process leads to 1,3-oxazines, that are key scaffolds in drug design,8–11 i.e. 1,3-benzoxazines with potent antibacterial, antifungal and antitumoral activities, among others, have been described.9,11 On the other hand, bioorganometallic chemistry has undergone a quick and spectacular growth in the last few decades, leading to organometallic compounds with relevant, and often new applications.12,13 The incorporation of metallocenes or, to a lesser extent, half-sandwich units into the structure of bioactive molecules or drugs is one of the most promising strategies in new drug discovery and in Medicinal Organometallic Chemistry (MOC).14 The spectacular achievements attained with ferrocene-based compounds15–18 [i.e. ferroquine16 (antimalarial agent now in clinical phase II trials), ferrocifens (potent antitumoral agents)] and other derivatives with remarkable antibacterial, antifungal, anti-VIH activities, among others15–18 have enhanced interest on complexes with "[M(η5-C5H4)(CO)3]" units, [M = Re (cyrhetrenyl) or Mn (cymantrenyl)]. Lipophilic and stable derivatives with interesting electrochemical and photo-physical properties18 and low toxicity are attractive in MOC.

Cyrhetrene and cymantrene chemistry has undergone a huge development in the last decade.19–22 New small molecules holding these "[M(η5-C5H4)(CO)3]" (M = Re or Mn) arrays attached to the backbones of commercially available drugs (i.e. chloroquine, nifurtimox, daunorubicin)19c and biomolecules (i.e. nucleobases and19a,b peptides22d–f) or with scaffolds of biological relevance (i.e. sulfones20b and heterocycles20f) are becoming more and more popular.19–21 Compounds of this kind with outstanding biological activities have been reported.19–21 The chloroquine conjugates I and II (Fig. 1) have a potent inhibitory growth effect in Trypanosoma brucei [IC50 = 3.5 μM (for I) and 0.6 μM (for II)].20d Sulphonamides III with better antitubercular activity than their ferrocenyl analogues are known.20b The cyrhetrenyl derivative IV has higher inhibitory growth potency on Trypanosoma cruzi epimastigotes (Dm28c strains) (IC50 = 2.4 μM) than those of compound V (IC50 = 12.3 μM) and nifurtimox (IC50 = 19.8 μM).20b Imines VI and VII are capable of inhibiting the growth of MCF7, MB-MDA231, and HCT116 cancer cell lines. Compound VII, (more active than VI), is two times more potent than cis-[PtCl2(NH3)2] (cisplatin) in MDA-MB231 and HCT116 colon cell lines.20i In fact, nowadays cyrhetrenyl and cymantrenyl derivatives are among the most promising candidates to achieve new drugs, more efficient and less toxic than those currently used to treat diseases causing high mortality (i.e. Chagas, malaria and cancer). Despite of this, and increasing interest on: (a) tautomeric equilibria shown in Scheme 1, (b) 1,3-benzoxazine derivatives, that may form via a 6-endo trig process and, (c) ferrocene,

cyrhetrene and cymantrene derivatives with bioactive arrays in MOC, compounds of this kind showing this sort of ring-chain tautomerism are scarce.5–7 Only three articles have been reported so far.5–7 Two involve a five-endo trig process that transforms imines (1 or 3 in Fig. 2) into their closed forms (2 and 4),5,6 while the third is the 6-endo trig process (shown in Fig. 2), involving 5a and 2-ferrocenyl-2,4-dihydro-1H-3,1-benzoxazine (6a).7 As far as we know, parallel studies on cyrhetrene or cymantrene derivatives have not been undertaken so far.

In this work, we present the first two examples of 2,4-dihydro-1H-3,1-benzoxazines with the [M(η5-C5H4)(CO)3] {M = Re or Mn} units on position 2; together with experimental and theoretical studies aimed to clarify the effect of the four substituents {ferrocenyl (a), phenyl (b), cyrhetrenyl (c) and cymantrenyl (d)} and the solvents on the stability of the imines [R{–CHvN-(C6H4-2-CH2OH)}] (5a–d), their closed tautomers (6a–d) and the tautomeric equilibria 5(a–d) ↔ 6(a–d).

Results and discussion

Synthesis

The treatment of equimolar amounts of cyrhetrenylcarboxaldehyde [Re(η5-C5H4-CHO)(CO)3]23 and 2-aminobenzylalcohol in benzene under reflux for 12 h using a Dean–Stark apparatus to remove the benzene–water azeotrope formed in the course of the reaction produced a colorless solution. Further concentration to dryness followed by successive washings of the residue with n-hexane gave a pale yellowish solid (herein after referred to as 6c). Its high resolution mass spectrum (Fig. S1†) showed a peak at m/z = 470.0394 that is consistent with that of the cation {[M] + H}+ (m/z = 470.0402) formed from any of the two tautomers [the imine (5c) or its closed form (6c)]. The IR spectrum of 6c (Fig. S2†) showed typical bands due to the CO ligands of the cyrhetrenyl unit (in the range 1900–2100 cm−1)20l and an intense and sharp absorption at 3325 cm−1, due to the stretching of the N–H bond, that is characteristic of 2,4-dihydro-1H-3,1-benzoxazines.6,8,11 These findings suggested that the isolated solid was 2-cyrhetrenyl-2,4-dihydro-1H-3,1-benzoxazine (6c in Scheme 2) and the X-ray diffraction studies (described below) confirmed it.

In contrast to these results, when the reaction was carried out under identical experimental conditions, but using [Mn(η5-C5H4-CHO)(CO)3],24 the 1H-NMR spectrum of the raw material isolated after concentration and successive washing with n-hexane at room temperature (Fig. S3†) revealed the coexistence of at least four species in solution, two of them being the starting reagents. The singlet observed at δ = 8.01 suggested the presence of the imine form (5d). The set of resonances assigned to the major component were consistent with those expected for 2-cymanthrenyl-2,4-dihydro-1H-3,1-benzoxazine (6d) depicted in Scheme 2. Since this reaction was performed under identical conditions used for the ferrocenyl, phenyl and cyrhetrenyl aldehydes, the results obtained from the NMR studies suggest that [Mn(η5-C5H4-CHO)(CO)3] is less prone to react with the aminoalcohol compared to its Re(I) analogue, or even to the ferrocenyl- or phenyl-aldehydes. Despite these findings, the complete reaction of the aldehyde [Mn(η5-C5H4-CHO)(CO)3] with the aminoalcohol was successfully achieved using an excess (20%) of the aldehyde and longer refluxing periods (24 h). Further purification of the crude material by SiO2 column chromatography gave a pale brownish solid. Mass spectra showed a peak (Fig. S4†) at m/z =338.0220, which agrees with those expected for the {[M] + H}+ cations (m/z = 338.0225) of both tautomers. The IR spectrum of 6d also showed the band due to the stretching of the N–H bond (at 3322 cm−1), quite close to that detected in the spectrum of its Re(I) analogue, 6c (at 3325 cm−1) and slightly shifted in relation to that of the ferrocenyl analogue (6b) (at 3348 cm−1). These results suggest that the isolated solid was the closed form 6d (Fig. S5†), and X-ray diffraction studies (see below) confirmed this finding.

For comparison purposes (see below) we also studied the reactions between the aldehydes [M(η5-C5H4-CHO)(CO)3] (M = Re or Mn) and 2-aminophenol under identical experimental conditions to 6c (see the

Experimental section). In the two cases, the isolated products were identified as the imines [M{(η5-C5H4)-CHvN-(C6H4-2-OH)}(CO)3] (with M = Re (7c) or Mn(7d)).

Characterization of the compounds

Compounds 6c and 6d were isolated as greenish (6c) or brownish (for 6d) crystals and show high stability in the solid state at room temperature. They are soluble in common solvents (i.e. CH3CN, CH2Cl2, CHCl3, ethyl acetate, benzene, dimethyl sulfoxide,and even mixtures of DMSO : H2O). These products were characterized in the solid state and also in solution. In the two cases elemental analyses (see the Experimental section) were consistent with the calculated values for their proposed formulae.

Their HRMS (Fig. S1 and S4A†) showed a peak at m/z = 470.0394 (for 6c) and at 338.0220 (for 6d), that agree with those expected for the corresponding {[M] + H}+ cation and their EI-mass spectra [Fig. S1B (for 6c) and S4B† (for 6d)] showed the peaks due to the cations [M]+; [M − CO]+; [M − 2CO]+ and [M − 3CO]+. The melting points of 6c and 6d are higher than those of their ferrocenyl- and phenyl-analogues (6a and 6b, respectively) and follow the trend: 6a (96 °C) < 6b (119 °C) < 6d (120 °C) < 6c (148 °C).

Description of the crystal structures

Compounds 6c and 6d were also characterized by X-ray diffraction and for comparison purposes we also crystallized and solved the crystal structure of the ferrocenyl derivative (6a) whose synthesis was reported previously6 (Table S1†). It should be noted that: (a) two different molecules (hereinafter referred to as A and B) were found in the crystals of 6c and, (b) in 6a the atoms of the C5H5 ring of the ferrocenyl unit were found in disordered positions. In all cases, the crystal structures confirmed the existence of the 2,4-dihydro-1H-3,1-benzoxazine array with a ferrocenyl (in 6a, Fig. 3), a cyrhetrenyl (in 6c, Fig. 4) or a cymantrenyl (in 6d, Fig. 5) group attached to position 2. Bond lengths and angles of the 1,3-N,O heterocycle in compounds 6a, 6c and 6d (Table 1) are very similar (the differences do not clearly exceed 3σ), and agree with the values found in related 2-phenyl substituted derivatives described previously.25,26 The non-planar oxazine rings27 exhibit a distorted half-chair conformation in 6a and a slightly distorted envelope-type in 6c (molecules A and B) and in 6d.28

In all cases, the heteroatoms O1 and N1 are located on opposite sides of the plane defined by the C5H4 ring. The O1 atom deviates from this plane by ca. 0.30 Å (in 6a); 0.42 Å and 0.63 Å (in molecules A and B of 6c) and 0.70 Å (in 6d) towards the metal centre. However, the separations O1···M 3.709 Å (in 6a), 3.732 Å and 3.750 Å (in molecules A and B, respectively of 6c) and 3.724 Å (in 6d) are greater than the sum of their van der Waals radii.29

The substituted pentagonal rings of the organometallic array are planar and twisted in relation to the phenyl ring of the bicyclic system, angles between their main planes being 55.05° (in 6a); 68.47° and 34.7° (in molecules A and B of 6c) and 68.07° in 6d. Bond lengths and angles of the (η5-C5H5)Fe (η5-C5H4) unit of 6a agree with those reported for most monosubstituted ferrocene derivatives.25

The assembly of the molecules in the crystals is complex due to the existence of a wide variety of intermolecular interactions. In the three cases, the hydrogen atom of the >NH unit plays a key role in the assembly of the molecules. In 6a and 6d the relative orientation of this H atom and the phenyl ring of a vicinal molecule allows their assembly by N–H···π interactions. In 6c, proximal molecules of the same type (A or B) are also connected due to these intermolecular short contacts.

The relative arrangement of the units in the crystals of 6a, 6c and 6d also allows C–H···π interactions, for instance between one of the H atoms of the –CH2– unit [H13B] and the unsubstituted ring of the ferrocenyl unit of a proximal molecule in 6a. For the cymantrenyl derivative (6d), the separation between the C6–H6 bond and the centroid of the ring defined by a set of atoms C(7)–C(12) is 2.85 Å. This suggests the existence of C–H···π intermolecular contacts. In 6c, these contacts involve the C6–H6 bond of molecule A at (x, y, z) and the phenyl ring of a B type unit located at (1 − x, 1 − y, −1/2 − z) and vice versa, assembling molecules A and B in the crystals.Moreover, in the cyrhetrenyl and cymantrenyl derivatives, additional CO···H intermolecular contacts30 between one oxygen of the CO ligands [O2 (in 6c) and O3B in 6c (molecule B)] or two [O3B and O4B (in type B molecules)] and one hydrogen atom of the C5H5 ring of a proximal molecule31 extend the assembly of the molecules in the crystals of 6c and 6d.

Characterization in solution

NMR studies have been a useful tool not only to characterize the new compounds in solution, but also: (a) to test their stability in solution, especially in the solvents used for the electrochemical and biological studies described below, (b) to evaluate the effect of the solvent on the ring-chain tautomerism of the new products and (c) to establish the influence of the nature of the four substituents R2 on the tautomeric equilibrium between imines 5a–5d and their closed forms (6a–6d). For all these studies the identification of the protons follows the pattern presented in Fig. S6.†

Proton-NMR spectra of freshly prepared solutions of 6c and 6d in acetonitrile-d3 (Fig. S7 and S8†) showed a set of two doublets and two triplets assigned to the aromatic protons (H3–H6) and a group of four complex multiplets due to the protons of the C5H4 ring. The remaining resonances observed in the spectra (doublet, a doublet of doublets and a broad signal) are characteristic of the protons of the >CH–, the –OCH2 and the NH units of the six-membered 1,3-N,O heterocycle, thus indicating that the closed forms (6c or 6d, respectively) were present in this solvent at room temperature. A careful analysis of the

1H-NMR spectra of 6c and 6d revealed the existence of another set of resonances with low intensity (Fig. S7 and S8,† respectively) indicating the presence of a minor component in acetonitrile-d3 at 298 K. The presence of a singlet in the range $8.00 < \delta < 8.20$ ppm suggested the presence of the imine forms 5c and 5d. Integration of the well-separated doublet due to one of the protons of the –OCH2– moiety of 6c (or 6d) of the imine protons of 5c (at $\delta = 8.16$ ppm) (or 5d at $\delta = 8.14$ ppm) (Fig. S7 and S8†) allowed us to determine the relative abundance of the tautomers in acetonitrile-d3 (molar ratios 6c : 5c ≈ 1.00 : 0.02 and 6d : 5d ≈ 1.00 : 0.04) (we will return to this point later on).

In order to fulfil the characterization of the new compounds in this solvent we also registered their 13C{1H}-NMR spectra (Fig. S9 and S10†). The assignment of the resonances observed in the 1H and 13C{1H}-NMR spectra was achieved with the aid of two-dimensional NMR experiments {ESI: [1H–1H]-NOESY (Fig. S11 and S12), [1H–13C]-HSQC (Fig. S13 and S14) and [1H–13C]-HMBC (Fig. S15 and S16)†}. In the [1H–1H]-NOESY spectra the cross-peaks between the signals due to protons of the –CH2– unit and one of the doublets observed in the aromatic region allowed the assignment of the signal due to the H3′ proton. Besides that, the identification of the signals due to the protons (H2 and H5) on the ortho sites of the (η5-C5H4) ring and to the H6′ was carried out on the basis of the NOE peaks involving these protons and those of the >CH–NH– unit.

These NMR studies revealed that the closed forms (6c and 6d) were the major components present in acetonitrile-d3 solutions at 298 K and coexisted with small amounts (<3.0%) of their corresponding imine forms: [R{–CHv(N-C6H4-2-CH2OH)}] (5c and 5d, respectively). Therefore, under these experimental conditions the tautomeric equilibrium is strongly shifted towards the 2-cyrhetrenyl (6c) or the 2-cymantrenyl (6d) -2,4-dihydro-1H-3,1-benzoxazine derivatives.

Electrochemical studies

As mentioned above, 1,3-benzoxazines and their derivatives have a wide range of applications, in which their electrochemical properties are a keystone, for instance their use or transformation to achieve resins or polymers.8,32 Moreover, it is well-known that their proclivity to undergo an oxidation process in biological media is also relevant in view of their utility in new drug design and development.8,11,33 In view of these findings, we also studied the electrochemical properties of the new compounds (6c and 6d) and compared them with those of the ferrocenyl- (6a) and phenyl- (6b) analogues (previously reported) under identical experimental conditions. The comparison of the results obtained for products 6a–6d may allow the elucidation of the effect of the four substituents (a–d) on position 2 on their electrochemical properties.

In all cases the electrochemical studies were carried out by cyclic voltammetry. The solvent selected for these studies was acetonitrile because of the fact that (a) NMR studies in acetonitrile-d3 confirmed the

stability of the products in this solvent, and, (b) it is well-known that the nature of the products formed by the oxidation of 1,3-benzoxazines is strongly dependent on the solvent and additives.8,32 Oxidation in acetonitrile produces preferentially radicals, which may have a key role in the biological medium [e.g. formation of reactive oxygen species (ROS)] and the metabolic degradation of 1,3-benzoxazines.8,33

Cyclic voltammetries of freshly prepared (10−3 M) solutions of the corresponding compounds (6a–6d) in acetonitrile (HPLC-grade) with (Bu4N)[PF6] as the supporting electrolyte were carried out at 298 K and a scan rate υ = 250 mV s−1. The cyclic voltammograms (hereinafter referred to as CV) are shown in Fig. 6 and a summary of the electrochemical data is presented in Table 2.

The CV of 6a shows the typical anodic peak (I) and its corresponding reduction one in the reverse scan (I′) between −1.2 V and 0.6 V. These peaks [with EI pa = 0.107 V and EI′ pc = 0.032 V], not observed in the CV of 6a–6d, are due to the electrochemical one electron oxidation–reduction of the ferrocenyl unit.

In all cases the voltammograms showed above 0.5 V another anodic peak (hereinafter referred to as II), which according to the bibliography could be attributed to the oxidation of the benzoxazine unit.8,32 The position of this peak is strongly dependent on the nature of the substituent and moves to the anodic region according to the sequence 6b < 6d < 6c ≪ 6a. This reflects a decrease of proclivity of the benzoxazine array to undergo the oxidation process. It should be noted that for 6a, this electrochemical process takes place after the oxidation of the ferrocenyl unit. This may explain the strong shift (to higher potentials) of peak II of 6a in comparison to those of 6b, 6c and 6d. At higher potentials the cyclic voltammograms of compounds 6b–6d show a broad and poorly defined peak (III).

For 6c and 6d, the additional oxidation peaks at around 1.2 V (labelled as IV in Fig. 6) are assigned (according to the bibliography) to further oxidation processes involving Re(I) (in 6c) or Mn(I) in 6d.8,19b,20e–i,22i,34,35 For the Re(I) complex the position of this peak appears at lower potentials than for imine [Re(η5-C5H4-CHvN-R2)(CO)3] VII as shown in Fig. 1 [with Epa = 1.420 V (under identical experimental conditions)].20h This suggests that the replacement of the ferrocenyl unit of VII by the 2,4-dihydro-1H-3,1-benzoxazine scaffold to give 6c enhances the proclivity of Re(I) to undergo oxidation.20i For 6d, the peak due to the oxidation of Mn(I) appears at higher potentials than for [Mn(η5-C5H5)(CO)3] (E = 0.92 V),34 but within the range (1.00 V–1.37 V) reported for cymantrene derivatives with substituted triazoles attached to the pentagonal C5H4 ring.22i

Study of the stability of the compounds 6c–6d and 7c–7d in solution and the effect of the solvent on the tautomeric equilibrium

It is well-known that for 2-aryl substituted benzoxazines, the ratio between the closed form and its open chain tautomer depends on several factors, of which the electronic nature of the substituent and the properties of the solvent are probably those with greater relevance.

To elucidate whether the tautomeric equilibria could be tuned by the solvent, further 1H-NMR studies were undertaken at 298 K in several deuterated solvents (CD2Cl2, C6D6 and DMSO-d6) with different polarities and dielectric constants.36 In all cases, the compounds were dissolved in the deuterated solvent and the solution was allowed to stand for some time to be sure that the equilibrium was reached. The relative abundance of the closed (6) and open (5) forms in each case was determined as described above (see Characterization in solution).

1H-NMR spectra of the solutions of compounds 6c and 6d in CD2Cl2 (Fig. S17 and S18†) also revealed that the closed forms were the major components present in solution and coexisted with tiny amounts of the imine forms in molar ratios quite similar to those obtained in acetonitrile-d3. Moreover, these studies revealed that new compounds (6c and 6d) are clearly more stable in CD2Cl2 than their analogues with ferrocenyl- of phenyl-derivatives for which 1H-NMR studies revealed the presence of greater amounts of the open forms (5a and 5b) (Fig. S19 and S20†), even after short periods of storage at 298 K, than for their cyrhetrenyl and cymantrenyl analogues. Moreover, as the storage period increased, the typical singlets due to ferrocenecarboxaldehyde (for 6a) {or to a minor extent also benzaldehyde (for 6b)} were also detected by NMR, thus indicating the low stability of the aldimines 5a and 5b in this solven

In contrast to the results obtained in acetonitrile-d3 and CD2Cl2, in benzene-d6, (Fig. S21 and S22†) no evidence of the presence of the imine forms was observed in any of the two cases, thus suggesting that the equilibrium is strongly displaced towards the closed forms (6c and 6d). This is markedly different to that observed for their ferrocenyl analogue, for which the closed (6a) and open (5a) forms co-existed in a molar ratio: 6a/5a = 1.1. Therefore the replacement of the ferrocenyl unit by the [M(η5-C5H4)(CO)3] arrays favours the displacement of the tautomeric equilibria towards the closed forms.

Finally, it should be noted that additional NMR studies of the solutions of compounds 6c and 6d in DMSO-d6 did not reveal the presence of the imine forms. Moreover, no significant difference was observed in the spectra of the freshly prepared solutions and those recorded after different periods of storage at 298 K (Fig. S25 and S26†). This indicates that both compounds also exhibit high stability in DMSO-solutions.

NMR spectra of compounds 7c and 7d, in CDCl3 (Fig. S27 and S28†), showed a set of signals, whose intensities and chemical shifts were consistent with those expected for the imines [M{(η5-C5H4)-CHvN-(C6H4-2-OH)}(CO)3] with M = Re (7c) or Mn (7d). For these products no evidence of the

presence of any other species in solution could be detected by 1H-NMR. These findings indicate that imines 7c and 7d are not prone to undergo the formation of the 1,3 N,O heterocycle through a 5-endo trig process. In contrast to the results obtained for 6c and 6d, 1H-NMR spectra of freshly prepared solutions of 7c and 7d at 298 K changed with time (Fig. S29 and S30†). After 4 h of storage, the spectrum of 7c showed an additional singlet at $\delta \approx 9.6$ ppm, which is indicative of the presence of free cyrhetrenylcarboxaldehyde. For the Mn analogue (7d), the spectrum obtained after 4 h was more complex and showed additional sets of signals with low intensity that suggested the presence of several species in solution. As shown in Fig. S30† after 24 h of storage the spectrum showed low resolution due to the broadening of the signals. The comparison of the results obtained for 7c and 7d reveals that both decompose gradually in DMSO-d6 at 298 K. For the Mn(I) derivative (7d) the process is faster and more complex than for its Re(I) analogue 7c. These findings are markedly different from those observed for their benzoxazine analogues 6c and 6d, for which their 1H-NMR spectra in DMSO-d6 did not show any significant change after long periods of storage at the same temperature.

Theoretical studies

In a first attempt to rationalize the influence of the organometallic array on ring-chain tautomerism, we decided to undertake DFT calculations for the open forms (5a–5d) and their corresponding tautomers (6a–6d). Theoretical calculations were performed at the B3LYP hybrid functional37 using the LANDL2DZ (for Re and Mn)38 and the 6-31G*39 (for the remaining atoms) basis set implemented in the Gaussian 03 software.40 The geometries of the open forms [R{–CHvN-(C6H4-2-CH2OH)}] (5a–5d) and their closed tautomers (6a–6d) were optimized. Final atomic coordinates for the optimized geometries are presented in Tables S2–S9.†

Optimized geometries of the open forms (5a–5d) revealed the existence of an intramolecular interaction between the imine nitrogen and the pendant –OH arm (Table S10†). It is well-known that for 2-phenyloxazolidines the influence of the substituents on the aryl ring on position 2 on the stability of the tautomers is controlled by several factors of which the intramolecular O–H···N bond appears to be especially relevant. The formation of the heterocycle requires the cleavage of the O–H···N bond and proper orientation between the oxygen on the –OH group and the imine carbon. Consequently, imines with weaker O–H···N bonds and closer O and Cimine atoms are expected to be more prone to undergo the 6-endo trig process.

In imines 5a–5d, the –OH bond lengths are quite similar [in the range 0.973 Å (for 5b) and –0.977 Å (for 5a)]. For compounds 5a, 5c and 5d with the (η5-C5H4) attached to the imine carbon, the N···H distance increases as follows: 1.959 Å (for 5a) $\ll$ 2.023 Å (for 5c) < 2.027 Å (for 5d). This suggests that in the ferrocenyl derivative (5a) the N···H interaction is stronger than in the cyrhetrenyl (5c) and cymantrenyl (5d) analogues and therefore less prone to undergo the formation of the closed form. This

agrees with the results obtained from the NMR studies described above, which proved the co-existence of the closed (6) and open (5) forms in acetonitrile-d3 or CD2Cl2 solutions at 298 K in different molar ratios that increased according to the sequence: 6a/5a ≪ 6c/5c < 6d/5d.

In order to gain further insight into this tautomeric process and after the optimization of the geometries of the open (5a–5d) and closed forms (6a–6d), we compared the electronic energy (ET) of the imines (5a–d) and their tautomers (6a–6d) in a vacuum as well as in CH2Cl2 solutions and in both cases, the ET values obtained for the closed forms were clearly lower than those of their corresponding imine forms (Table S11†).

The solution studies described above showed that in CD2Cl2 the molar ratios 6d/5d and 6c/5c were greater than those observed for the set of compounds holding a phenyl (b) or a ferrocenyl (a) unit, indicating that the presence of the cyrhetrenyl or cymantrenyl units shifts the tautomeric equilibrium towards the closed forms. In view of this, additional computational studies were carried out in order to determine the free energy of the open (5a–d) and closed (6a–d) forms in CH2Cl2 at 298 K. The comparison of the results [Table S11,† A] reveals that the imine forms are less stable compared to their tautomers with identical substituents. Moreover, for the three organometallic pairs of compounds with a (η5-C5H4) ring attached to the imine carbon in the open forms (5) or to position 2 of the benzoxazines in the closed tautomers (6), the comparison of the values of the free energy for the process 6i → 5i [ΔGi, defined as: ΔG(for 5i)–ΔG(for 6i)] (with identical substituent i = a, c or d) [see Table S11,† B] increases according to the sequence a < c < d. This trend suggests that compounds 6c and 6d with [M(η5-C5H4)(CO)3] (M = Re or Mn) units are less prone to undergo a ring opening process compared to their ferrocenyl analogue 6a. This could explain the greater abundance of the closed forms 6c or 6d detected in CD2Cl2 solutions at 298 K solution, when compared to that of 6a. Moreover, it is well known that the stability of ferrocenylimines in solution is strongly dependent on the solvent used and its quality. Traces of water or acids present in CD2Cl2 or CDCl3 solutions frequently promote their hydrolysis.39,20i,41 Compounds of general formulae [(η5-C5H5)Fe{(η5-C5H4)-CHvN-R}] with phenyl groups attached to the imine nitrogen are less prone to hydrolysis compared to their analogues with alkylic substituents, and a similar phenomenon has also been described for the hybrid ferrocenyl/cyrhetrenyl derivative [(η5-C5H5)Fe{(η5-C5H4)-CHvN-(η5-C5H4)Re(CO)3}] (VI, in Fig. 1).20i Degradation of the aldimine 5a is expected to shift the equilibrium 6a ↔ 5a towards the right and this explains the coexistence of 6a, 5a and [Fe(η5-C5H5){(η5-C5H4)-CHO}], (formed by the hydrolyses of 5a) after several hours of storage of a solution of 6a in CD2Cl2 at 298 K (Fig. S19†).

The comparison of the frontier orbitals of the closed forms 6a–6d can be useful to clarify the effect of the substituents on the electronic distribution of molecular orbitals; we also undertook molecular orbital calculations for the closed forms 6a–6d. Frontier orbitals [HOMO−1, HOMO, LUMO and LUMO+1] are depicted in Fig. 7. For compounds 6a, 6c and 6d, HOMO−1 is mainly centred on the corresponding

organometallic fragments; while in their phenyl analogue in 6b, it is basically located on the phenyl ring of the bicyclic system with a tiny contribution of the –OCH2– unit and the remaining C6H5 ring. Except for compound 6a, in which the atomic orbitals of the Fe(II) ion have a significant contribution on the HOMO orbital, for 6b–6d it is mainly centred on the aromatic ring of the benzoxazine array and the heterocyclic nitrogen, without any significant participation of the organometallic "[M(η5-C5H4)(CO)3]" units of 6c and 6d. However, the replacement of the phenyl ring of 6b by the cyrhetrenyl- or cymantrenyl-arrays (in 6c and 6d), respectively, is important to modify the relative contribution of the atomic orbitals in their HOMO and especially that of the nitrogen. Therefore, the oxidation of compounds 6b–6d requires the removal of one electron on the HOMO orbital centred on the bicyclic system. The energy of their HOMO orbitals increases according to the sequence: 6b < 6c < 6d. (Table S12†), but it should be noted that these calculations were performed under vacuum and therefore no solvent effects were included in this calculation. This may explain the differences observed between the trend of their E(HOMO) and the experimental EII pa values (obtained from cyclic voltammetries in acetonitrile).

As shown in Fig. 7 the LUMO is basically a π* orbital of the ferrocenyl (in 6a), the [M(η5-C5H4)] units of 6c or 6d or the two phenyl rings of 6b. The LUMO+1 orbital is located on the organometallic units of compounds 6a, 6c and 6d, while in 6b it is a combination of π* orbitals of the two phenyl rings.

We also compared the energies of the HOMO and LUMO orbitals and the values of their energy gaps (Egap) for compounds 6a–6d. As shown in Table S12,† the values of Egap increase according to the sequence 6d < 6c < 6a < 6b. This should affect the position of the band detected in the absorption spectra due to the transition HOMO → LUMO. ESI contains the UV-vis spectra of the complexes in CH2Cl2 at 298 K (Fig. S31) and a summary of UV-vis data is presented in Table S13.†

Due to increasing interest of fused rings containing heteroatoms with good donor abilities as ligands for transition metals, a comparative analysis of the charge distribution on the heterocycle was also carried out. The results presented in Table S12† reveal that the nature of the substituent produces significant variations in the calculated charges of the carbon and oxygen atoms of the "CH2–O–CH" unit. For compounds 6a, 6b and 6c the charge on the nitrogen is very similar, but all of them are smaller than that obtained for their Mn(I) analogue (6d). This difference may be important in view of its reactivity and potential capability to be used as a ligand in front of transition metals.

Biological studies

As mentioned above organometallic compounds with fac-[M (η5-C5H5)(CO)3] cores and 3,1-benzoxazine derivatives are attractive in view of their utility in new drug design. The new compounds 6c and 6d presented in this work contain both units simultaneously and coexist in solution with small

amounts of their open forms 5c and 5d. Moreover, it is wellknown that Schiff bases may also exhibit interesting biological activities. For instance, compound VI presented in Fig. 1 and other aldimines of general formulae: [(η5-C5H5)Fe{(η5-C5H4)-CHvN-R}] with potent anticancer activities have been reported. 20i,42 In view of these, we also decided to perform additional studies in order to evaluate their biological activities as anticancer or as anti-parasitic agents

1H-NMR studies (described above) of the ferrocenyl- or the phenyl-derivatives (6a and 6b, respectively) and also the new imines [M{(η5-C5H4)-CHvN-(C6H4-2-OH)}(CO)3] {M = Re (7c) or Mn (7d)} demonstrate that: (a) 6a and 6b exhibit low stability in solution due to the hydrolyses of their open form tautomers (5a and 5b); (b) compound 7c decomposes in DMSO-d6 at 298 K and the degradation of its Mn analogue (7d) is even faster and more complex than that of 7c under identical experimental conditions. Unfortunately, these findings reduce significantly their potential for new drug design, and this is the main reason why compounds 6a, 6b, 7c and 7d were not included in the biological studies described in this section.

In a first stage, in vitro studies on the effect produced by the new compounds 6c and 6d on the same set of cancer cell lines used before for imines VI and VII (shown in Fig. 1) were performed. The effects of 6c and 6d on HCT-116 (colon), the MDA-MB231 and the MCF7 breast cancer cell lines and of cisplatin, used as the positive control, were assessed after 72 h and the results are presented in Table 3 and Fig. 8.

In the HCT-116 cell line the Mn(I) derivative (6d) resulted to be less potent compared to its Re(I) analogue (6c), but their inhibitory growth potency was clearly smaller than that of cisplatin. For the triple negative (ER, PR and no HER overexpression) MDA-MB231 breast cancer cell line, the results (Fig. 8 and Table 3) were even worse than in HCT-116. Neither 6c nor 6d showed any relevant activity (IC50 > 100 μM). However, parallel studies on MCF-7 revealed that the Re(I) compound (6c) has a greater antiproliferative effect than its Mn(I) analogue (6d), but its potency is clearly smaller than those of the reference drug and imine VII (IC50 = 12 ± 5.2 μM).20i

We also undertook a comparative study of the effect of the new products (6c and 6d) on the normal and non-tumoral human skin fibroblast BJ cell line. The results obtained (Fig. 9) reveal that the Re(I) derivative (6c) [IC50 = 65.3 ± 2 μM] is a bit less toxic compared to its Mn(I) analogue 6d [IC50 = 52.6± 2 μM] and both exhibit a lower inhibitory growth effect than cisplatin (IC50 = 21 ± 2 μM) under identical experimental conditions. This finding together with the high stability of the new compounds is particularly attractive for further studies centred on their biological activities in other areas.

In view of the results obtained from the in vitro cytotoxic activity of the compounds in the cancer cell lines, and especially in the normal and non-tumoral BJ cells we focused our attention on their evaluation as potential antiparasitic agents. With this aim in mind, the Trypanosoma cruzi epimastigotes (Dm28c strain) were incubated with various concentrations of compounds 6c and 6d and for comparison

purposes a parallel study with nifurtimox (one of the drugs used currently in the treatment of Chagas diseases) was also undertaken under identical experimental conditions. As shown in Fig. 10 despite the formal similarity between 6c and 6d, their inhibitory growth effect on the selected strain of parasites was markedly different. The Re(I) complex (6c), the more potent anticancer agent than 6d on HCT-116 and MCF7, showed no significant anti-Trypanosoma cruzi activity (Fig. 10). In contrast to these results 6c exhibited antiparasitic activity with an inhibitory growth potency greater than that of the aldimine [Re{(η5-C5H4)-(CH2)-NvCHR}(CO)3] with R = 5-nitrofurane (IC50 = 87.7 ± 2.1 μM) and practically identical to that of the 4-nitrothiophene analogue (IC50 = 43.1 ± 0.8 μM), but clearly below that of nifurtimox (IC50 = 17.4 ± 0.3 μM under identical conditions) and the Re(I) complex IV presented in Fig. 1 (IC50 = 2.4 μM).20b

Since compounds 6c and 6d have an identical set of organic ligands and a 2,4-dihydro 3,1-benzoxazine unit connected to the [M(η5-C5H4)(CO)3] units, they differ exclusively in the nature of the M(I) atom [M = Re(I) (in 6c) or Mn(I) (in 6d)]. The results obtained from these biological studies reveal that the replacement of Re(I) of 6c by Mn(I) to give 6d is important as to induce significant variations in their antichagasic activity. This finding is in sharp contrast to the previous results summarized in a recent review as follows: “if the metaltricarbonyl core is covalently bound to an organic molecule the obtained antiparasitic activity is mainly dependent on the nature of the non-metallic portion of the compound”.13a

It is well-known that the oxidation of benzoxazines constitutes one of the initial steps in their metabolic degradation.8,32 The electrochemical and computational studies presented here show that oxidation of 6c and 6d requires the removal of one electron from their HOMO which is centred on the benzoxazine core in both cases, and that for 6d this process occurs at lower potentials than for its Re(I) analogue (6c) [EIIpa = 0.615 (for 6d) versus 0.702 (for 6c)] and therefore more accessible in the biological media. On this basis the Mn(I) complex is more prone to oxidize than its Re(I) analogue and this may produce radicals and even reactive oxygen and nitrogen species (ROS and RNS) that play an important role in cell survival, for instance as signalling molecules regulating the neutrophil function.

Conclusions

The two first examples of an unprecedented type of organometallic 2-substituted 2,4-dihydro-1H-3,1-benzoxazines with [M(η5-C5H4)(CO)3] arrays and M = Re (6c) or Mn (6d) at position-2 have been prepared and characterized in the solid state and also in solution. NMR and electrochemical studies of 6c, 6d and their ferrocenyl (6a) or phenyl (6b) analogues (previously reported) have allowed us to establish the influence of the substituents [ferrocenyl (a), phenyl (b), cyrhetrenyl (c) or cymantrenyl (d)] on the ease with which benzoxazines 6a–6d undergo: (a) the ring opening process to give 5a–5d and (b) oxidation.

Theoretical studies based on DFT and TD-DFT methodologies for 5a–5d and 6a–6d have allowed us to elucidate the effect of the substituents on the relative stability {in a vacuum and in CH2Cl2 solution} and the electronic distribution of the closed 6a–6d and open forms 5a–5d. These calculations have been extremely useful to understand the different proclivities of the closed forms (6a–6d) to undergo the opening of the sixmembered 1,3 N,O heterocycle to give their imine partners (5a–5d).

The results obtained from the biological studies demonstrate that the replacement of the Re(I) of 6c by Mn(I) to give 6d induces significant changes in their biological activities. The Re(I) complex 6c, with no significant antichagasic activity, showed a moderate inhibitory growth effect on the MCF7 cancer cell line, while its Mn(I) analogue (6c) (inactive in the cancer cells) exhibited moderate anti-Trypanosoma cruzi activity. Despite the fact that the inhibitory growth effects of 6c in the MCF7 cancer cell line or of 6d in the Dm28c strain are far from those of cisplatin or nifurtimox respectively, their remarkable stability (in the solid state and in DMSO solutions) at 298 K and their low toxicity in normal and non-tumoral BJ cell lines make them extremely attractive for further studies aimed to check their effect on other cancer cell lines and/or other parasites (i.e. as antimalarials). Besides, the results summarized here open up a bunch of new possibilities based on: (a) substitution of the CO ligands by phosphines, (b) their utility as ligands in front of transition metal ions or (c) the extension of the methods reported here to half-sandwich complexes with other transition metals (i.e. Cr, Tc), with different properties, activities and potential utilities.

In addition, since benzoxazine derivatives are becoming more and more popular as precursors for the preparation of resins or polymers, the new compounds presented here may also be attractive from this point of view. The presence of the "[M(η5-C5H4)(CO)3]" cores [M = Re(I) (in 6c) or Mn(I) (in 6d)] may be useful to achieve new types of organometallic resins and/or polymers.

Experimental

Materials and methods

The aldehydes [M(η5-C5H4-CHO)(CO)3] with M = Re or Mn and compounds 6a and 6b were prepared as described previously. 6,23,24 The aminoalcohols H2N-C6H4-2-(CH2)nOH (n = 1 or 0) were purchased from Sigma-Aldrich and used as received. The preparation of the new compounds requires the use of benzene as a solvent, which should be used with CAUTION! This solvent as well as ethyl acetate (HPLC-grade) were obtained from commercial sources and used as received, and the remaining solvents (n-hexane and CH2Cl2) used during the synthesis and purification of the compounds were purified using the standard methods.43 The deuterated solvents used for the NMR studies were purchased from Sigma-Aldrich (benzene-d6 (99.9%) and CD2Cl2 (99.9%)) or from Acros-Organics [acetonitrile-d3 (99.95%), CDCl3 (99.8%) or DMSO-d6 (99.5%)]. All manipulations were performed under an N2 atmosphere using Schlenk techniques.

High resolution mass spectra (HRMS) were recorded at the Servei d' Espectrometría de Masses (Univ. Barcelona) using a LC/MSD-TOF Agilent Technologies instrument and electron impact (EI) mass spectra were obtained with a Shimadzu CC-MS spectrometer (70 eV) at the Laboratorio de Servicios Analíticos (Pontificia Universidad Católica de Valparaiso). C, H and N analyses were performed with an Eager 1108 microanalyzer. Infrared (IR) spectra of the new compounds were registered with a Nicolet 400 FTIR instrument using KBr pellets. Proton and 13C{1H}-NMR spectra of the new products in acetonitrile- d3 were recorded at 298 K with a Mercury 400 MHz instrument. These NMR data are presented in the characterization section of the corresponding compound and the spectra are shown in Fig. S7–S10.† The assignment of the signals detected was achieved with the aid of two-dimensional NMR experiments: [1H–1H]-Nuclear Overhauser Effect Spectroscopy (Fig. S11 and S12†) (NOESY), [1H–13C] Heteronuclear Single Quantum Coherence Spectroscopy (HSQC) (Fig. S13 and S14†) and Heteronuclear Multiple-Bond Correlation Spectroscopy (HMBC) (Fig. S15 and S16†).

Additional 1H-NMR studies of the new compounds in CD2Cl2 (Fig. S17 and S18†), and of their ferrocenyl and phenyl analogues (Fig. S19 and S20†) and complementary studies [in benzene-d6 (Fig. S21 and S22†) and DMSO-d6 (Fig. S25 and S26†)] together with 13C{1H}-NMR studies of 6c and 6d in benzene and CD2Cl2 (Fig. S23 and S24†) were also carried out at 298 K in order to elucidate the effect induced by these solvents on the tautomeric equilibria and to fulfill the characterization of 6c and 6d in solution. NMR spectra of imines 7c and 7d in CDCl3 at 298 K (Fig. S27 and S28,† respectively) and the studies of their stability in DMSO-d6 and after several periods of storage were carried out at 298 K (Fig. S29 and S30,† respectively). In all cases, chemical shifts (δ) are given in ppm and the coupling constants (J) in Hz. The assignment of the resonances observed refers to the labelling patterns presented in Fig. S6† and the abbreviations for the multiplicities of the signals are as follows: s (singlet), d

(doublet), t (triplet), m (multiplet), dd (doublet of doublets) and br (broad). Finally, the ultraviolet-visible (UV-vis) spectra of 1 × 10−5 M solutions of compounds 6a–6d in CH2Cl2 were recorded with a CARY 100 scan Varian UV spectrometer at 298 K (Fig. S31†).

Preparation of the compounds

2-Cyrhetrenyl-2,4-dihydro-1H-3,1-benzoxazine (6c). Cyrhetrenylcarboxaldehyde (100 mg, 0.275 mmol) and the stoichiometric amount of 2-aminobenzylalcohol (33.9 mg, 0.275 mmol) were suspended in 20 mL of benzene. The flask was connected to a condenser equipped with a Dean–Stark apparatus, to remove the benzene–water azeotrope formed and the reaction mixture was stirred under reflux for 12 h. After this period, the hot solution was concentrated to dryness on a rotary evaporator. Further treatment of the residue formed with n-hexane gave the corresponding compound as pale greenish microcrystals. [Yield: 116 mg, 0.25 mmol, 90%]. Characterization data: M.p. = 148° C; mass spectrum (Fig. S1†): HRMS (m/z): 470.0394 and calc. for {[M] + H}+(C16H12NO4Re): 470.0402 and EI-MS: (based on 187Re): m/z = 469, [M]+; 441 {[M] − CO}+; 413 {[M] − 2CO}+ and 385 {[M] − 3CO}+. IR (selected data) (in cm−1): 3324 [ν(CvN)], 2019 [ν(CO)] and 1905 [ν(CO)]. 1H-NMR data [in acetonitrile-d3, (400 MHz) at 298 K (Fig. S7†)]: δ1H, 7.07(t, 1H, J = 8.1, H4), 6.94 (d, J = 7.5, H3), 6.78(t, 1H, J = 7.5, H5), 6.71(d, 1H, J = 7.6, H6), 5.72–5.68[2m(partially overlapped), 2H, H2 and H5], 5.36(d, 1H, J = 4.0, H8), 5.49(m, 1H, H4), 5.45(m, 1H, H3), 4.97(d, 1H, J = 14.1, H7), 4.78(d, 1H, J = 14.1, H7) and 4.74[br. 1H, –NH– (partially overlapped by the resonance due to one of the protons H7]; 13C{1H}-NMR data [in acetonitrile-d3 (125 MHz), at 298 K (Fig. S9†)]: δ13C = 195.3(CO), 142.5(C2), 127.5(C4), 124.9(C3), 122.6(C1), 119.4(C5), 116.7(C6), 109.4(C1), 84.9(C4), 84.4(C2), 83.5(C5), 84.1(C3), 79.2(C8), 66.7(C7). Anal. (%) calcd for C16H12NO4Re: C, 41.02; H, 2.58 and N, 2.99. Found: C, 41.0; H, 2.6 and N, 3.0

2-Cymantrenyl-2,4-dihydro-1H-3,1-benzoxazine (6d). 2-Aminobenzylalcohol (53.1 mg, 0.431 mmol) was added to a solution of cymantrenylcarboxaldehyde (120 mg, 0.517 mmol) in 20 mL of benzene. The flask was connected to a condenser equipped with a Dean–Stark apparatus to remove the benzene–water azeotrope formed, and the mixture was refluxed for 24 h. After this period, the hot solution was concentrated to dryness on a rotary evaporator. The residue was dissolved in a minimum amount of ethyl acetate. The work up of SiO2 column chromatography on silica gel (eluent n-hexane : ethyl acetate, 90 : 10) produced the release of a band that was collected and concentrated to dryness giving a gummy residue. 1H-NMR spectra of this residue revealed the coexistence of compound 6d and traces of the aldehyde. This minor component was removed by subsequent washings of the residue with n-hexane. Finally, the brownish dust powder isolated was dried under vacuum. [Yield: 103.2 mg, 0.30mmol, 71%]. Characterization data: M.p. = 120° C; mass spectrum (Fig. S4†): HRMS: m/z =

338.0220 and calc. for: {[M] + H}+(C16H13MnNO4): 338.0225 and EI-MS: (based on 55Mn): m/z = 337 [M]+; 309 {[M] − CO}+; 281 {[M] − 2CO}+; 253 {[M] − 3CO}+. IR selected data (KBr; cm−1): 3322 [ν(N–H)], 2019 [ν(CO)] and 1932 [ν(CO)]. 1H-NMR data [in acetonitrile-d3, (400 MHz) at 298 K (Fig. S8†)]: δ1H = 7.10(t, 1H, J = 8.1, H4), 6.78(d, 1H, J = 7.5, H3), 6.75(t, 1H, J = 8.0, H5), 6.72(d, 1H, J = 8.0, H6), 5.32(d, 1H, J = 4.6, H8), 5.09–5.07[2m(partially overlapped) 2H, H2 and H5], 4.97(d, 1H, J = 14.8, one of the protons H7), 4.90–4.70(br. m, 3H, –NH–, H3 and H4), 4.79(d, 1H, J = 14.8, the other H7); 13C{1H}-NMR data [in acetonitrile-d3 (125 MHz), at 298 K, (Fig. S10†)]: δ13C = 142.6(C2), 128.2(C4), 125.3(C3), 122.5(C1), 120.2(C5), 117.5(C6′), 105.2(C1), 80.5(C7), 67.8(C8), 84.9 and 84.4(C2 and C5), 84.1 and 83.3(C3 and C4).44 Anal. (%) calcd for C16H12MnNO4: C, 56.99; H, 3.59 and N, 4.15. Found: C, 56.9; H, 3.6 and N, 4.1.

Compounds [M{(η5-C5H4)-CHvN-(C6H4-2-OH)}(CO)3] (7) {M = Re (7c) or Mn (7d)}. These new cyrhetrenyl and cymantrenyl imino complexes were prepared as described above for 6c. For compound 7c: 2-aminophenol (22.5 mg, 0.21 mmol) and the aldehyde [Re(η5-C5H4-CHO)(CO)3] (75 mg, 0.21 mmol) were dissolved in benzene (20 mL). Then the reaction flask was connected to a Dean–Stark apparatus and refluxed for 12. Afterwards, the solvent was removed under vacuum and the solid formed was washed with small portions of n-hexane and then dried under vacuum. Imine 7d was prepared following the same procedure but using cymantrenylcarboxaldehyde (75 mg, 0.32 mmol) and 35.3 mg (0.32 mmol) of 2-aminophenol. Compounds 7c and 7d were finally isolated as yellow microcrystals and as a nearly black solid, respectively. [Yields: 80.1 mg (0.18 mmol, 86%) for 7c and 52.2 mg (0.16 mmol, 50%) for 7d]. Characterization data for 7c: M.p. = 107° C; mass spectrum: HRMS (m/z): 456.0240 calc. for {[M] + H}+ (C15H11NO4Re): 456.0241 and EI-MS (based on 187Re): m/z = 455, [M]+; 427 {[M] − CO}+; 399 {[M] − 2CO}+ and 371 {[M] − 3CO}+. IR (selected data) (in cm−1): 2015 [ν(CO)], 1941 [ν(CO)] and 1633 [ν(CvN)]. 1H-NMR data [in CDCl3, (400 MHz) at 298 K]: δ1H = 8.32(s, 1H, –CHvN–), 7.19[m, 2H, H4 and –OH (overlapped signals)], 6.99(dd, 1H, J = 8.1 and 1.3, H6), 6.88(td, 2H, J = 7.5 and 1.2, H5 and H3), 6.02(t, 2H, J = 2.3, H2 and H5), 5.46(t, 2H, J = 2.3, H3 and H4). 13C{1H}-NMR data [in CDCl3, (101 MHz), at 298 K]: δ13C = 192.7(CO), 152.0(–CHvN–), 149.5 (C2), 134.9(C1), 129.5(C4), 120.4(C3), 116.1(C5), 115.4(C6), 98.7 (C1), 86.5(C2 and C5) and 85.0(C3 and C4). Characterization data for 7d: M.p. = 90° C; mass spectrum: HRMS (m/z): 324.0063, calc. for {[M] + H}+ C15H11NO4Mn: 324.0063 and EI-MS (based on 55Mn): m/z = 323, [M]+; 295 {[M] − CO}+; 267 {[M] − 2CO}+ and 239 {[M] − 3CO}+. IR (selected data) (in cm−1): 2022 [ν(CO)], 1930 [ν(CO)] and 1623 [ν(CvN)]. 1H-NMR data [in CDCl3, (400 MHz) at 298 K]: δ1H, 8.29(s, 1H, –CHvN–), 7.18[m, 2H, H4 and –OH (overlapped signals)], 6.99 (dd, 1H, J = 8.3 and 0.9, H6), 6.88(m, 2H, H5 and H3), 5.45 (broad triplet, 2H, H2 and H5) and 4.90(broad triplet, 2H, H3 and H4).

Crystallography

X-ray crystals of compounds 6a, 6c and 6d were obtained by slow evaporation (at 298 K) of a CH2Cl2 solution of the corresponding product layered with n-hexane. A crystal of 6a, 6c or 6d (sizes in Table S1†) was used for the X-ray analysis. X-ray intensity data were measured on a D8 Quest system (for 6a) or on a D8 Venture system (for 6c and 6d) equipped with a multilayer monochromator and a Mo-microfocus (λ = 0.71073 Å).

For 6a, 6c and 6d the frames were integrated with a Bruker SAINT software package using a narrow frame algorithm. The integration of data using a monoclinic (for 6a), an orthorhombic (for 6c) or a monoclinic (for 6d) unit cell yielded for 6a: a total of 16 003 reflections to a maximum θ angle of 26.416° (0.72 Å resolution), of which 2941 were independent (average redundancy 3.338, completeness = 99.6%, Rint = 2.58%, Rsig = 2.36%). For 6c, which was a twin crystal, a total of 25 066 reflections to a maximum θ angle of 29.554° (0.72 Å resolution) of which 7511 were independent (average redundancy 3.337, completeness = 99.7%, Rint = 4.02%, Rsig = 4.60%); and for 6d: 35 346 reflections to a maximum θ angle of 30.174° (0.71 Å resolution) of which 4058 were independent (average redundancy 8.710, completeness = 99.4%, Rint = 9.07%, Rsig = 5.17%). The number of reflections greater than 2σ(F2) was: 2831 (for 6a), 6741 (for 6c) and 3228 (for 6d).

The final cell parameters for 6a, 6c and 6d presented in Table 1 are based upon the refinement of XYZ centroids of reflections above 20 σ(I). Data were corrected for absorption effects using the multi-scan method (SADABS). The calculated minimum and maximum transmission coefficients based on crystal sizes are given in Table 1.

The structures were solved and refined using the Bruker SHELXTL software package using the space group P21 (for 6a), Pna21 (for 6c) and C2/c (for 6d) (Z = 8 in both cases) for the formula units C18H17NOFe (in 6a) and C16H12NO4M {M = Re (in 6c) or Mn (in 6d)}. The final anisotropic full-matrix leastsquares refinements on F2 with 165 variables (for 6a), 386 for 6c and 199 for 6d converged at R1 = 2.29%, (observed data) and wR2 = 5.45% (for all data) for 6a; at R1 = 3.59%, (observed data) and wR2 = 8.22% (all data) for 6c and at R1 = 4.58%, (observed data) and wR2 = 12.27% (all data) for 6d. The goodness of fit and further details concerning the resolution and refinement of the crystal structures of 6a, 6c and 6d are presented in Table S1.† CCDC 1858655 (for 6a), 1858656 (for 6c) and 1858654 (for 6d)† contain the supplementary crystallographic data for this paper.25

Electrochemical studies

Cyclic voltammetric (CV) studies were carried out at room temperature using a Metrohm Autolab potentiostat and a three-electrode cell. Each compound was dissolved in acetonitrile containing 0.1 mol L−1 of tetrabutylammonium hexafluorophosphate (Bu4N)[PF6] as a supporting electrolyte to give 10−3 mol L−1 final concentration. A 2 mm platinum working electrode and a platinum coil counter electrode were used. The reference electrode contained a silver wire with 10 mM silver nitrate in (Bu4N)[PF6] electrolyte solution.

The working electrode was polished with 0.3 and 0.05 μm alumina slurries, rinsed with distilled water (18 MΩ cm) and acetone, and dried prior to use. All electrolyte solutions were thoroughly pre-purged using purified nitrogen gas before use. The measurements were carried out at 250 mV s−1 scan rate. The ferrocene/ferricinium (Fc/Fc+) couple served as the internal reference and appeared at +89 mV (vs. Ag/Ag+) for each experiment.

Computational studies

DFT calculations were carried out using Gaussian 03 software40 with the B3LYP functional.37 The basis set was chosen as follows: LANL2DZ (for Fe, Re and Mn) and 6-31G* (including polarization functions for non-hydrogen atoms) for O, N, C and H.39 Geometry optimizations were performed without symmetry restrictions. Solvent effects have been included using the CPCM method.45

Biological studies

Cell culture. Colon adenocarcinoma (HCT116) cells (from the American Type Culture Collection) and breast cancer (MDA-MB231 and MCF7) cells (from European Collection of Cell Cultures, ECACC) were used for all the experiments. The cells were grown as a monolayer culture in DMEM-high glucose (Sigma, D5796) in the presence of 10% heat-inactivated fetal calf serum and 0.1% streptomycin/penicillin under standard culture conditions. The human skin fibroblast cell line BJ was cultured in MEM (Sigma, M2279) in the presence of 10% FBS, 4 mM glutamine and 0.5% streptomycin/penicillin. All the cells were incubated under standard conditions (humidified air with 5% CO2 at 37 °C). The cells were passaged at 90% confluence by washing once with cation-free HBSS followed by a 3 min incubation with trypsin ([0.5 μg mL−1]/EDTA [0.2 μg mL−1]) (Gibco-BRL, 15400054) solution in HBSS at 37 °C, and transferred to its medium. Prior to seeding at a defined cell concentration, the cells were recovered from the medium by centrifugation and counted.

Cell viability assays. For these studies, compounds 6c and 6d were dissolved in 100% DMSO at 50 mM as stock solution; then, consecutive dilutions have been done in DMSO (1 : 1) (in this way DMSO concentration in cell media was always the same); followed by 1 : 500 dilutions of the solutions of compounds on cell media. Cisplatin was dissolved in water Milli-Q® and used immediately after its preparation. The assay was carried out as described by Givens et al.46 In brief, MDA-MB231 and MCF7 cells were plated at 5000 cells per well or 10 000 cells per well respectively, in 100 μL media in tissue culture 96 well plates (Cultek). BJ cells were plated at 2500 cells per well. After 24 h, the medium was replaced by 100 μL per well of serial dilution of drugs. Each point concentration was run in triplicate. Reagent blanks, containing media plus colorimetric reagent without the cells, were run on each plate. Blank values were subtracted from test values and were routinely 5–10% of uninhibited control values. Plates were incubated for 72 h. Hexosaminidase activity was measured according to the following protocol: the media containing the cells were removed and the cells were washed once with phosphate buffer saline (PBS) and 60 μL of substrate solution (7.5 mM p-nitrophenol-N-acetyl-β-D-glucosamide [Sigma N9376], 0.1 M sodium citrate, pH = 5.0, 0.25% Triton X-100) was added to each well and incubated at 37 °C for 1–2 h; after this incubation time, a bright yellow colour appeared; then, plates could be developed by adding 90 μL of developer solution (glycine 50 mM, pH = 10.4; EDTA 5 mM), and absorbance was recorded at 410 nm.

In vitro anti-trypanosomal activity

Parasites. Trypanosoma cruzi, epimastigotes (Dm28c strain), from our own collection (Clinical and Molecular Pharmacology Program, Institute of Biomedical Sciences (ICBM), Faculty of Medicine, University of Chile), were grown at 28 °C in LIT medium, with 4 μM hemin, supplemented with inactive 10% v/v FBS, 100 U mL−1 penicillin, and 100 mg mL−1 streptomycin at 28 °C. The parasites were harvested and collected for viability.

Anti-proliferative assays. All compounds were dissolved in DMSO (final concentration was less than 0.5% v/v) at a concentration range (1–100 μM), added to a suspension of epimastigotes (3 × 106 parasites per mL) and incubated for 24 h at 37 °C. Nifurtimox was added as a positive control. Later, MTT47 was added at a final concentration of 0.5 mg mL−1 with phenazine methosulfate (0.22 mg mL−1) and incubated at 37 °C for 4 h. The parasites were solubilized in 10% sodium dodecyl sulfate–0.01 M HCl and incubated overnight beforedetermining the number of viable parasites. The optical density (OD) was determined using a microplate reader (Asys Expert Plus©, Austria) at 570 nm. Under these conditions, the OD is directly proportional to the viable cell number in each well. All experiments were performed in triplicate and data are shown as the means and their standard deviations from

693 triplicate cultures. The IC50 values were obtained using non-linear dose–response curve fitting analysis
694 (log of concentration vs percentage of viable cells) via Graph Pad Prism 5 software.48

695

Acknowledgements

A. H. K. and R. A. acknowledge FONDECYT-Chile (projects 1150601 and 11130443), FONDEQUIP EQM 130154 and D. I. Pontificia Universidad Católica de Valparaiso; J. O. is grateful to CONICYT-PFCHA for a doctoral scholarship number 21170802 and D.I.-PUCV; C. P. S. acknowledges Proy. POSTDOC_DICYT-USACH (021740PI PostDoc). This work was also supported by the Ministerio de Economía y Competitividad of Spain [Grant number CTQ-2015-65040P (subprogram BQU)]. Authors also acknowledge Prof. J. D. Maya and Dr Michel Lapier from the School of Medicine of Universidad de Chile, for their collaboration in the antichagasic studies. We also thank Dr Mauricio Fuentealba for X-Ray diffraction assistance.

References

R. E. Valters and W. Flitsch, Ring-chain Tautomerism, Plenum Press, New York, USA, 1985.

(a) R. E. Valters, F. Fülöp and D. Korbonits, Adv. Heterocycl. Chem., 1996, 66, 1–71 (b) J. Elguero, A. R. Katritzky and O. Denisko, Adv. Heterocycl. Chem., 2000, 76, 1–84; (c) B. Stanovnik, M. Tišler, A. R. Katritzky and O. V. Denisko, Adv. Heterocycl. Chem., 2006, 91, 1–134; (d) I. Szatmari, T. A. Martinek, L. Lázár, A. Koch,E. Kleinpeter, K. Neuvonen and F. Fülöp, J. Org. Chem., 2004, 69, 3645–3653; (e) L. Lázár and F. Fülöp, Eur. J. Org. Chem., 2003, 3025–3042 and references cited therein.

R. Krieg, R. Wrywa, U. Möllman, H. Görls and B. Schönecker, Steroids, 1998, 63, 531–541.

Selected articles on ring-chain tautomerism involving 1,3-N,O heterocycles: (a) A. M. García-Deibe, C. Portela-García, M. Fondo and J. Sanmartín-Matalobos, RSC Adv., 2015, 5, 58327–58333; (b) L. Guasch, M. Sitzmann and M. C. Nicklaus, J. Chem. Inf. Model., 2014, 54, 2423–2432; (c) M. Juhász, L. Lázár and F. Fülöp, Tetrahedron: Asymmetry, 2011, 22, 2012–2017; (d) K. Pihlaja, M. Juhász, H. Kivelä and F. Fülöp, Rapid Commun. Mass Spectrom., 2008, 22, 1510–1518.

B. Shafaatian, M. Hashemibagha, B. Notash and S. A. Rezvani, J. Organomet. Chem., 2015, 791, 51–57.

D. Talancón, R. Bosque and C. López, J. Org. Chem., 2010, 75, 3294–3300.

S. Pérez, C. López, A. Caubet, A. Roig and E. Molins, J. Org. Chem., 2005, 70, 4857–4860.

L. Lázár and F. Fülop, in Comprehensive Heterocyclic Chemistry III, ed. A. R. Katritzy, C. A. Ramsden, E. F. Schriver and R. J. Taylor, Elsevier, Oxford, 2008, vol. 8, pp. 373–459.

For a general overview on this area see also: (a) R. D. Kamble, S. V. Hese, R. J. Meshram, J. R. Kote, R. N. Gacche and B. S. Dawane, Med. Chem. Res., 2014, 24, 1077–1088; (b) E. Abele, R. Abele, L. Golomba, J. Visnevska, T. Beresneva, K. Rubina and E. Lukevics, Chem. Heterocycl. Compd., 2010, 46, 905–930; (c) T. J. Sindhu, S. D. Arikkatt, G. Vincent, M. Chandran, A. R. Bhat and K. Krishnakumar, Int. J. Pharm. Sci. Res., 2013, 4, 134–143; (d) J. B. Chylinska, T. Urbanski and M. Mordarski, J. Med. Chem., 1963, 6, 484–487; (e) M. E. Kuehne and E. A. Konopka, J. Med. Chem., 1962, 5, 257–280.

Selected and recent contributions on this area: (a) A. M. Thompson, P. D. O'Connor, A. J. Marshall, V. Yardley, L. Maes, S. Gupta, D. Launay, S. Braillard, E. Chatelain, S. G. Franzblau, B. Wan, Y. Wang, Z. Ma, C. B. Cooper and W. A. Denny, J. Med. Chem., 2017, 60, 4212–4233; (b) M. R. M.

De Brito, W. J. Peláez, M. S. Faillace, G. C. G. Militao, J. R. G. S. Almeida, G. A. Arguello, Z. Szakonyi, F. Fülöp, M. C. Salvadori, F. S. Teixeira, R. M. Freitas, P. L. S. Pinto, A. C. Mengarda, M. P. N. Silva, A. A. Da Silva and J. De Moraes, Toxicol. In Vitro, 2017, 44, 273–279.

See for instance: (a) N. Siddiqui, R. Ali, M. S. Alam and W. Ahsan, J. Chem. Pharm. Res., 2010, 2, 309–316; (b) A. A. Pawar, S. R. Butle, P. U. Pawar, V. P. Phulwale, K. V. Patawar, S. P. Upadhaye, K. M. Chilwant and S. M. Sarate, World J. Pharm. Res., 2016, 5, 556–570; (c) A. El-Mekabaty, Int. J. Mod. Org. Chem., 2013, 2, 81–121; (d) M. Akhter, S. Habibullah, S. M. Hasan, M. M. Alam, N. Akhter and M. Shaquiquzzaman, Med. Chem. Res., 2011, 20, 1147–1153; (e) D. Indorkar, O. P. Chourasia and S. N. Limaye, Res. J. Chem. Sci., 2016, 6, 25–31; (f) S. Kalra, A. Kumar and M. K. Gupta, Med. Chem. Res., 2013, 22, 3444–3451.

(a) Bioorganometallic Chemistry: Applications in Drug Discovery, Biocatalysis, and Imaging, ed. G. Jaouen and M. Le Salmain, Wiley-VCH, Weinheim, Germany, 2015; (b) Topics in Organometallic Chemistry: Bioorganometallic Chemistry, ed. G. Simonneaux, Springer, Heildelberg, Germany, 2006, vol. 17.

For review purposes see for instance: (a) D. Gambino and L. Otero, Inorg. Chim. Acta, 2018, 472, 58–75; (b) R. H. Fish, J. Organomet. Chem., 2015, 782, 3–16; (c) A. Simonneau, F. Le Bideau, J.-H. Mirebeau, J. Marrot and G. Jaouen, Curr. Top. Med. Chem., 2017, 17, 2807–2819; (d) B. Albada and N. Metzler-Nolte, Chem. Rev., 2016, 116, 11797–11839; (e) S. S. Rodrigues and C. C. Romao, Adv. Mater. Sci. Res., 2012, 5, 155–170; (f) J.-L. Duprey and J. H. Tucker, Chem. Lett., 2014, 43, 157–163; (g) M. A. Blackie, Mini-Rev. Med. Chem., 2013, 13, 597–606; (h) R. H. Fish and G. Jaouen, Organometallics, 2003, 22, 2166–2177; (i) S. El-Kazzouli, N. El-Brahmi, S. Mignani, M. Bousmina, M. Zablocka and J. P. Majoral, Curr. Med. Chem., 2012, 19, 4995–5010; (j) I. S. Butler, R. P. Kengne-Momo, A. Vessières, G. Jaouen and C. Policar, Appl. Spectrosc. Rev., 2012, 47, 620–632; (k) A. L. Noffke, A. Habtemariam, A. M. Pizarro and P. J. Sadler, Chem. Commun., 2012, 48, 5219–5246; (l) E. A. Hillard and G. Jaouen, Organometallics, 2011, 30, 20–27; (m) G. Gasser, I. Ott and N. Metzler-Nolte, J. Med. Chem., 2011, 54, 3–25; (n) R. H. Fish, Aust. J. Chem., 2010, 63, 1505–1513; (o) C. Biot and D. Dive, Top. Organomet. Chem., 2010, 32, 155–193; (p) N. Chavain and C. Biot, Curr. Med. Chem., 2010, 17, 2729–2745; (q) S. S. Rodrigues, Organometallic Compounds, ed. H. F. Chin, Organometalliccompounds in therapy: an expanding horizon, 2010, pp. 293–308; (r) C. G. Hartinger and P. J. Dyson, Chem. Soc. Rev., 2009, 38, 391–401.

(a) R. W. Brown and C. J. T. Hyland, Med. Chem. Commun., 2015, 6, 1230–1243; (b) G. Jaouen and P. J. Dyson, in Comprehensive Organometallic Chemistry III, ed. D. Mingos and R. Crabtree, Elsevier, Oxford, 2007, vol. 12, pp. 445–464; (c) M. P. Coogan, Organometallics, 2012, 31,

5671–5672; (d) G. Gasser and N. Metzler-Nolte, Curr. Opin. Chem. Biol., 2012, 16, 84–91; (e) P. J. Dyson, Chimia, 2011, 65, 730–733; (f) Topics in Organometallic Chemistry: Medicinal Organometallic Chemistry, ed. G. Jaouen and N. Metzler-Nolte, Springer, Heildelberg, Germany, 2010, p. 32.

P. Stepnicka, Ferrocenes: Ligands, Materials and Biomolecules, Wiley-VCH, Weinheim, Germany, 2008.

(a) F. A. Larik, A. Saeed, T. A. Fattah, U. Muqadar and P. A. Channar, Appl. Organomet. Chem., 2016, 31, 1–22; (b) C. Biot, Curr. Med. Chem.: Anti-Infect. Agents, 2004, 3, 135–147; (c) C. Roux and C. Biot, Future Med. Chem., 2012, 4, 783–797 and references therein.

See for instance: (a) E. R. Reddy, R. Trivedi, L. Giribabu, B. Sridhar, K. P. Kumar, M. S. Rao and A. V. S. Sarma, Eur. J. Inorg. Chem., 2013, 30, 5311–5319; (b) A. Burmudžija, Z. Ratković, J. Muškinja, N. Janković, B. Ranković, M. Kosanić and S. Đorđević, RSC Adv., 2016, 6, 91420–91430; (c) S. Realista, S. Quintal, P. N. Martinho, A. I. Melato, A. Gila, T. Esteves, M. de Deus Carvalho, L. P. Ferreira, P. D. Vaz and M. J. Calhorda, J. Coord. Chem., 2017, 70, 314–327.

(a) A. G. Ginzburg, Russ. Chem. Rev., 2009, 78, 195–210; (b) R. B. King, in Transition-Metal Organometallic Chemistry. An Introduction, Accademic press, New York, USA, 1969, pp. 93–110.

(a) A. Jabłoński, K. Matczak, A. Koceva-Chyła, K. Durka, D. Steverding, K. Jakubiec-Krześniak, J. Solecka, D. Trzybiński, K. Woźniak, V. Andreu, G. Mendoza, M. Arruebo, K. Kochel, B. Krawczyk, D. Szczukocki and K. Kowalski, Molecules, 2017, 22, 2220; (b) K. Kowalski, L. Szczupk, S. Saloman, D. Steverding, A. Jabłoński, V. Vrček, A. Hildebrandt, H. Lang and A. Rybarczyk-Pirek, ChemPlusChem, 2017, 82, 303–314; (c) E. V. Sharova, O. I. Artyushin, N. V. Vinogradova, G. K. Genkina and V. K. Brel, Mendeleev Commun., 2017, 27, 608–609; (d) I. A. Utepova, A. A. Musikhina and O. N. Chupakhin, Russ. Chem. Bull., 2016, 65, 2523–2558; (e) J. Hess, M. Patra, L. Rangasamy, S. Konatschnig, O. Blacque, A. Jabbar, P. Mac, E. M. Jorgensen, R. B. Gasser and G. Gasser, Chem. – Eur. J., 2016, 22, 16602–16612; (f) M. Patra, M. Wenzel, P. Prochnow, V. Pierroz, G. Gasser, J. E. Bandow and N. Metzler-Nolte, Chem. Sci., 2015, 6, 214–224; (g) V. Tirkey, S. Mishra, H. R. Dash, S. Das, B. P. Nayak, S. M. Mobin and S. Chatterjee, J. Organomet. Chem., 2013, 732, 122–129; (h) M. Patra, G. Gasser, M. Wenzel, K. Merz, J. E. Bandow and N. Metzler-Nolte, Organometallics, 2012, 31, 5760–5771.

(a) R. Arancibia, F. Dubar, B. Pradines, I. Forfar, D. Dive, A. H. Klahn and C. Biot, Bioorg. Med. Chem., 2010, 18, 8085–8091; (b) C. Quintana, G. Silva, A. H. Klahn, V. Artigas, M. Fuentealba, C. Biot, I. Halloum, L. Kremer, N. Novoa and R. Arancibia, Polyhedron, 2017, 134, 166–172; (c)

C. Echeverria, V. Romero, R. Arancibia, H. Klahn, I. Montorfano, R. Armisen, V. Borgna, F. Simon and R. Ramirez-Tagle, BioMetals, 2016, 29, 743–749; (d) R. Arancibia, A. H. Klahn, G. E. Buono-Core, E. Gutierrez-Puebla, A. Monge, M. E. Medina, C. Olea-Azar, J. D. Maya and F. Godoy, J. Organomet. Chem., 2011, 696, 3238–3244; (e) P. Toro, C. Suazo, A. Acuña, M. Fuentealba, V. Artigas, R. Arancibia, C. Olea-Azar, M. Moncada, S. Wilkinson and A. H. Klahn, J. Organomet. Chem., 2018, 862, 13–21; (f) J. Gómez, A. H. Klahn, M. Fuentealba, D. Sierra, C. Olea-Azar, J. D. Maya and M. E. Medina, J. Organomet. Chem., 2017, 839, 108–115; (g) J. Gómez, A. H. Klahn, M. Fuentealba, D. Sierra, C. Olea-Azar and M. E. Medina, Inorg. Chem. Commun., 2015, 61, 204–206; (h) M. Muñoz-Osses, F. Godoy, A. Fierro, A. Gómez and N. Metzler-Nolte, Dalton Trans., 2018, 47, 1233–1242; (i) J. Oyarzo, A. Acuña, A. H. Klahn, R. Arancibia, C. P. Silva, R. Bosque, C. López, M. Font-Bardía, C. Calvis and R. Messeguer, Dalton Trans., 2018, 47, 1635–1649; (j) J. Gómez, N. Leiva, R. Arancibia, J. Oyarzo, G. E. Buono-Core, A. H. Klahn, V. Artigas, M. Fuentealba, R. Bosque, G. Aullón, C. López, M. Font-Bardía and T. Calvet, J. Organomet. Chem., 2016, 819, 129–137; (k) T. Cautivo, A. H. Klahn, F. Godoy, C. López, M. Font-Bardía, T. Calvet, E. Gutierrez-Puebla and A. Monge, Organometallics, 2011, 30, 5578–5589; (l) S. Raju, C. Van Slagmaat, M. Lutz, H. Kleijn, J. Jastrzebski, M. Moret and R. Klein, Eur. J. Inorg. Chem., 2017, 741–751.

(a) L. Glans, W. Hu, C. Jöst, C. de Kock, P. J. Smith, M. Haukka, H. Bruhn, U. Schatzschneider and E. Nordlander, Dalton Trans., 2012, 41, 6443–6450; (b) W. Hu, K. Splith, I. Neundorf, K. Merz and U. Schatzschneider, J. Biol. Inorg. Chem., 2012, 17, 175–185. 22 (a) K. Lam, S. J. Van Wyck and W. E. Geiger, J. Electroanal. Chem., 2017, 799, 531–537; (b) M. Wenzel, M. Patra, C. H. Senges, I. Ott, J. J. Stepanek, A. Pinto, P. Prochnow, C. Vuong, S. Langklotz, N. Metzler-Nolte and J. E. Bandou, ACS Chem. Biol., 2013, 8, 1442–1450; (c) T. Dallagi, M. Saidi, G. Jaouen and S. Top, Appl. Organomet. Chem., 2013, 27, 28–35; (d) K. Splith, W. Hu, U. Schatzschneider, R. Gust, I. Ott, L. A. Onambele, A. Prokop and I. Neundorf, Bioconjugate Chem., 2010, 21, 1288–1296; (e) K. Splith, I. Neundorf, W. Hu, H. W. P. N'Dongo, V. Vasylyeva, K. Merz and U. Schatzschneider, Dalton Trans., 2010, 39, 2536–2545; (f) H. W. P. N'Dongo, I. Ott, R. Gust and U. Schatzschneider, J. Organomet. Chem., 2009, 694, 823–827; (g) H. W. P. N'Dongo, I. Neundorf, K. Merz and U. Schatzschneider, J. Inorg. Biochem., 2008, 102, 2114–2119; (h) I. Neundorf, J. Hoyer, K. Splith, R. Rennert, H. W. P. N'Dongo and U. Schatzschneider, Chem. Commun., 2008, 5604–5606; (i) D. P. Day, T. Dann, D. L. Hughes, V. S. Oganesyan, D. Steverding and G. G. Wildgoose, Organometallics, 2014, 33, 4687–4696.

J. M. Heldt, N. Fischer-Durand, M. Salmain, A. Vessières and G. Jaouen, J. Organomet. Chem., 2004, 689, 4775–4782.

837 M. Hromadová, M. Salmain, R. Sokolová, L. Pospísil and G. Jaouen, J. Organomet. Chem., 2003, 668,
838 17–24.

839 Cambridge Crystallographic Data Centre (CCDC) available online at
840 http:\\www.ccdc.cam.ac.uk/data_request/cif.

841 K. Patel, S. Deshmukh, D. Bodkhe, M. Mane, K. Vanka, D. Shinde, P. R. Rajamohanan, S. Nandi, R.
842 Vaidhyanathan and S. H. Chikkali, J. Org. Chem., 2017, 82, 4342–4351.

843 Deviations from the mean plane: in 6a, O1, −0.327; N1, −0.073; C6, +0.294; C7, −0.089; C12, +0.061;
844 and C13, +0.134 Å; in the two non-equivalent molecules of 6c: O1A, +0.352; N1A, 0.053; C6A,
845 −0.290; C7A, +0.096; C12A, +0.049; and C13A, −0.163 Å (molecule A); O1B, −0.353; N1B,
846 0.035; C6B, 0.277; C7B, −0.076; C12B, +0.042 and C13B, +0.175 Å (molecule B); and in 6d:
847 O1, +0.358; N1, +0.051; C6, −0.288; C7, +0.098; C12, −0.047; and C13, −0.172 Å.

848 Puckering analyses for 6a: φ = 202° and ϕ = 125°; for 6c: φ = 16° and ϕ = 54.2° (in A) and φ = 192° and
849 ϕ = 124° (in B) and for 6d φ = 195.1° and ϕ = 125.8°.

850 A. Bondi, J. Phys. Chem., 1964, 68, 441–451.

851 G. R. Desiraju and T. Steiner, The Weak Hydrogen Bond in Structural Chemistry and Biology, in IUCR
852 Monographs on Crystallography, Oxford University Press, Oxford, UK, 1999, vol. 9.

853 Analyses of potential hydrogen bonds for 6d between the C4–H4 bond of a molecule sited at (x, y, z)
854 and the O2 atom of another unit at (x, 1 − x, z) [D–H, 1.00 Å; H···A, 2.58 Å, D···A 3.38 Å]. For
855 6c: in molecule A: there is a short intermolecular contact between the C2A–H2A bond of the unit
856 at (x, y, z) and the O4 atom of another one at (x, 1 − y, z) (D–H, 1.00 Å; H···A, 2.56 Å and D···A
857 3.20 Å); while B, the C2B–H2B and the C4B–O3B of a type B-molecule at (x, y, z) are close to
858 the O4B and O3B atoms, respectively of two different units sited in (12 + x, 12− y, z) and (x, −1
859 + y, z) {D–H, 1.00 Å; H···A, 2.44 Å, D···A 3.13 Å and D–H, 1.00 Å; H···A, 2.60 Å, D···A, 3.37
860 Å, respectively}.

861 (a) H. Ishida and A. Agag, Handbook of Benzoxazine Resins, Elsevier, Oxford, UK, 2011, ch. 8, pp.
862 175–182; (b) S. K. S. Santhosh-Kumar and C. P. Reghunadhan-Nair, Polybenzoxazines:
863 Chemistry and Properties, Smithers Rapra Technology, 2010; (c) P. Audebert, A. Roche and J.
864 Pagetti, J. Electroanal. Chem., 1995, 383, 139–143.

865 (a) K. Nesmerak, I. Nemec, M. Sticha, K. Waisser and K. Palat, Electrochim. Acta, 2005, 50, 1431–
866 1437; (b) E. Baher and N. Darzi, Iran. J. Pharm. Res., 2017, 16, 146–157; (c) A. Toropov, K.
867 Nesmerak, I. Raska, K. Waisser and K. Palat, Comput. Biol. Chem., 2006, 30, 434–437.

868 D. R. Laws, J. Sheats, A. L. Rheingold and W. E. Geiger, Langmuir, 2010, 26, 15010–15021.

869 N. Agurto, T. Maldonado, F. Godoy, A. Gómez, C. P. Silva, J. Pavez, G. Ferraudi, A. Oliver and A. G.
870 Lappin, J. Organomet. Chem., 2017, 827, 32–40.

871 Dielectric constants (ε) and dipolar moments (μ, in D) ofthe solvents used in this study: benzene, ε =
872 2.27 and μ = 0.0; CH2Cl2, ε = 8.93 and μ = 1.55; acetone, ε = 37.5 and μ = 3.45 and dimethyl
873 sulphoxide, ε = 46.7 and μ = 3.9.

874 (a) A. D. Becke, J. Chem. Phys., 1993, 98, 5648–5652; (b) C. Lee, W. Yang and R. G. Parr, Phys. Rev.
875 B: Condens. Matter Mater. Phys., 1988, 37, 785–789.

876 (a) W. R. Wadt and P. J. Hay, J. Chem. Phys., 1985, 82, 284–298; (b) P. J. Hay and W. R. Wadt, J.
877 Chem. Phys., 1985, 82, 270–283; (c) P. J. Hay and W. R. Wadt, J. Chem. Phys., 1985, 82, 299–
878 310.

879 (a) P. C. Hariharan and J. A. Pople, Theor. Chim. Acta, 1973, 28, 213–222; (b) M. M. Francl, W. J.
880 Pietro, W. J. Hehre, J. S. Binkley, M. S. Gordon, D. J. DeFrees and J. A. Pople, J. Chem. Phys.,
881 1982, 77, 3654–3665.

882 M. J. Frisch, G. W. Trucks, H. B. Schlegel, G. E. Scuseria, M. A. Robb, J. R. Cheeseman, J. A.
883 Montgomery, T. Vreven, K. N. Kudin, J. C. Burant, J. M. Millam, S. S. Iyengar, J. Tomasi, V.
884 Barone, B. Mennucci, M. Cossi, G. Scalmani, N. Rega, G. A. Petersson, H. Nakatsuji, M. Hada,
885 M. Ehara, K. Toyota, R. Fukuda, J. Hasegawa, M. Ishida, T. Nakajima, Y. Honda, O. Kitao, H.
886 Nakai, M. Klene, X. Li, J. E. Knox, H. P. Hratchian, J. B. Cross, V. Bakken, C. Adamo, J.
887 Jaramillo, R. Gomperts, R. E. Stratmann, O. Yazyev, A. J. Austin, R. Cammi, C. Pomelli, J. W.
888 Ochterski, P. Y. Ayala, K. Morokuma, G. A. Voth, P. Salvador, J. J. Dannenberg, V. G.
889 Zakrzewski, S. Dapprich, A. D. Daniels, M. C. Strain, O. Farkas, D. K. Malick, A. D. Rabuck, K.
890 Raghavachari, J. B. Foresman, J. V. Ortiz, Q. Cui, A. G. Baboul, S. Clifford, J. Cioslowski, B. B.
891 Stefanov, G. Liu, A. Liashenko, P. Piskorz, I. Komaromi, R. L. Martin, D. J. Fox, T. Keith, M. A.
892 Al-Laham, C. Y. Peng, A. Nanayakkara, M. Challacombe, P. M. W. Gill, B. Johnson, W. Chen,
893 M. W. Wong, C. González and J. A. Pople, Gaussian 03 (Revision C.02), Gaussian, Inc.,
894 Wallingford, CT, 2004.

895 See for instance: (a) S. Pérez, C. López, A. Caubet, X. Solans and M. Font-Bardía, Eur. J. Inorg. Chem.,
896 2008, 1599–1612; (b) C. López, A. Caubet, S. Pérez, X. Solans and M. Font-Bardía, Chem.
897 Commun., 2004, 540–541; (c) A. Caubet, C. López, R. Bosque, X. Solans and M. Font-Bardia, J.
898 Organomet. Chem., 1999, 577, 292–304; (d) C. López, A. Caubet, X. Solans and M. Font-Bardía,
899 J. Organomet. Chem., 2000, 598, 87–102.

See for instance: (a) D. Talancón, C. López, M. Font-Bardía, T. Calvet, J. Quirante, C. Calvis, R. Messeguer, R. Cortés, M. Cascante, L. Baldomà and J. Badia, J. Inorg. Biochem., 2013, 118, 1–12; (b) J. Albert, R. Bosque, M. Crespo, J. Granell, C. López, R. Cortés, A. González, J. Quirante, C. Calvis, R. Messeguer, L. Baldomà, J. Badía and M. Cascante, Bioorg. Med. Chem., 2013, 21, 4210–4217.

D. D. Perrin and W. L. F. Amarego, Purification of Laboratory Chemicals, Butterworth–Heinemann, Oxford, UK, 4th edn, 1996.

In the 13C{1H} NMR spectrum of 6d in acetonitrile-d3, (Fig. S10), the resonances of the C2–C5 carbon atoms appeared in an extremely narrow range and in the 1H-NMR spectra (Fig. S8), the resonances of the protons attached to them were overlapped, as a consequence of these, some of the cross peaks observed in the 2D spectra were also overlapped (Fig. S12–S14 and S16) as a consequence, it was not possible to fulfil the assignment of signals due to these carbon atoms. Besides, the signals due to the quaternary carbon atoms of the CO groups were not observed in the spectrum (Fig. S6).†

M. Cossi, N. Rega, G. Scalmani and V. Barone, J. Comput. Chem., 2003, 24, 669–681.

K. T. Givens, S. Kitada, A. K. Chen, J. Rothschiller and D. A. Lee, Invest. Ophthalmol. Visual Sci., 1990, 31, 1856–1862.

S. Muelas, M. Suárez, R. Pérez, H. Rodríguez, C. Ochoa, J. A. Escario and A. Gómez-Barrio, Mem. Inst. Oswaldo Cruz, 2002, 97, 269–272.

http://utsavbali.com/wp-content/uploads/2013/10/Prism5 Regression.pdf.

Legends to figures

Scheme 1 Five- and six-endo trig processes (E = S or O).

Fig. 1 Selection of cyrhetrene and cymantrene derivatives with relevant antiparasitic or antitumoral activity described. (For comparison purposes, compound V, closely related to IV, has also been included.)

Fig. 2 Examples of ferrocene derivatives showing ring-chain tautomerism reported so far.5–7 For comparison purposes the 6-endo trig process of the aldimine 5b and its closed form (6b) is also included.

Scheme 2 Synthesis of the new compounds and six-endo trig process under study. (i) For M = Re: equimolar amount of the reagents in refluxing benzene with a Dean–Stark apparatus for 12 h and for M = Mn: treatment of the aminoalcohol with an excess (20%) of the aldehyde in benzene under reflux with a Dean–Stark apparatus for 24 h, followed by the work-up of SiO2 column chromatography using a mixture of ethyl acetate : hexane (10 : 90) as the eluent, followed by concentration and washings with n-hexane.

Fig. 3 ORTEP diagram for compound 6a. Thermal ellipsoids are shown at 50% probability level.

Fig. 4 ORTEP diagrams of molecules (A and B) found in the crystals of compound 6c. Thermal ellipsoids are shown at 50% probability level.

Fig. 5 ORTEP diagram for compound 6d. Thermal ellipsoids are shown at 50% probability level.

Fig. 6 Cyclic voltammograms of 2-[ferrocenyl, phenyl, cyrhetrenyl or cymantrenyl]-2,4-dihydro-1H-3,1-benzoxazines (6a–6d, respectively), in the range of potentials $-1.2\ V \leq E \leq 1.6\ V$, together with the labelling system used to identify the observed peaks. For the ferrocenyl derivative (6a) the cyclic voltammogram in the range $-1.2\ V \leq E \leq 0.6\ V$ is shown in grey color as an inset of the CV. The vertical dotted lines are presented for comparison purposes.

Fig. 7 Frontier orbitals [HOMO−1, HOMO, LUMO and LUMO+1] for the 2-ferrocenyl- (6a), phenyl- (6b), cyrhetrenyl- (6c) or cymantrenyl- (6d) 2,4-dihydro-1H-3,1-benzoxazines under study.

Fig. 8 Inhibition of cell growth proliferation in the colon (HCT-116) and breast (MDA-MB231 and MCF7) cancer cell lines after 72 h of exposure to 2-cyrhetrenyl- (6c) or cymantrenyl- (6d) 2,4-dihydro-1H-3.1-benzoxazines and cisplatin.

Fig. 9 Inhibition of cell growth proliferation in the normal and nontumoral human skin fibroblast BJ cell line of compounds 6c and 6d and cisplatin under identical experimental conditions.

Fig. 10 Effect of 2-cyrhetrenyl- (6c) or cymantrenyl- (6d) -2,4-dihydro-1H-3.1-benzoxazines and nifurtimox on the Trypanosoma cruzi epimastigotes (Dm28c strain).

SCHEME 1

5-endo trig *6-endo trig*

FIGURE 1

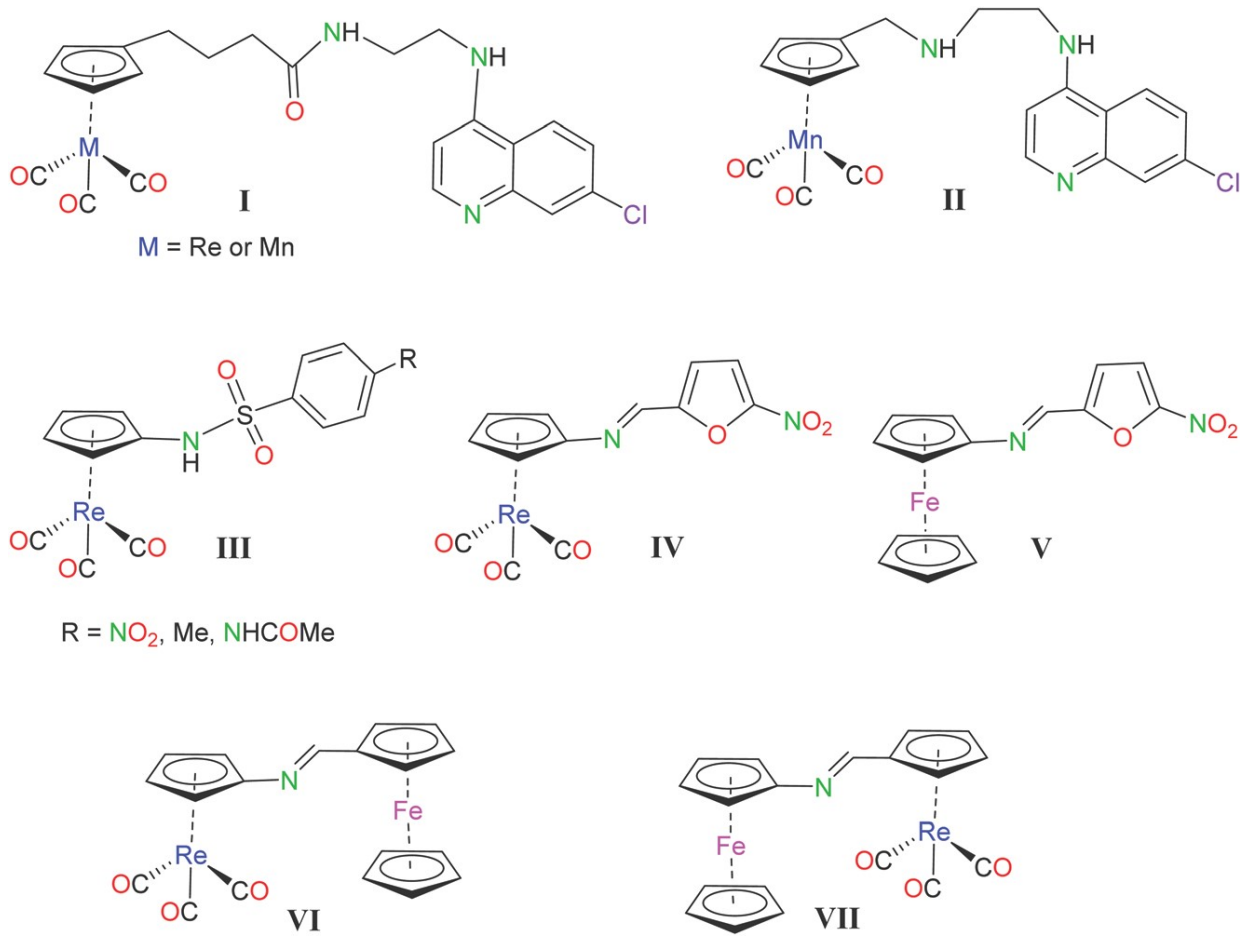
NH
NH
O
M
OC
CO
OC
I
N
Cl
M = Re or Mn
Mn
II
R
O
S
O
N
H
Re
III
R = NO2, Me, NHCOMe
NO2
IV
Fe
V
VI
VII

FIGURE 2

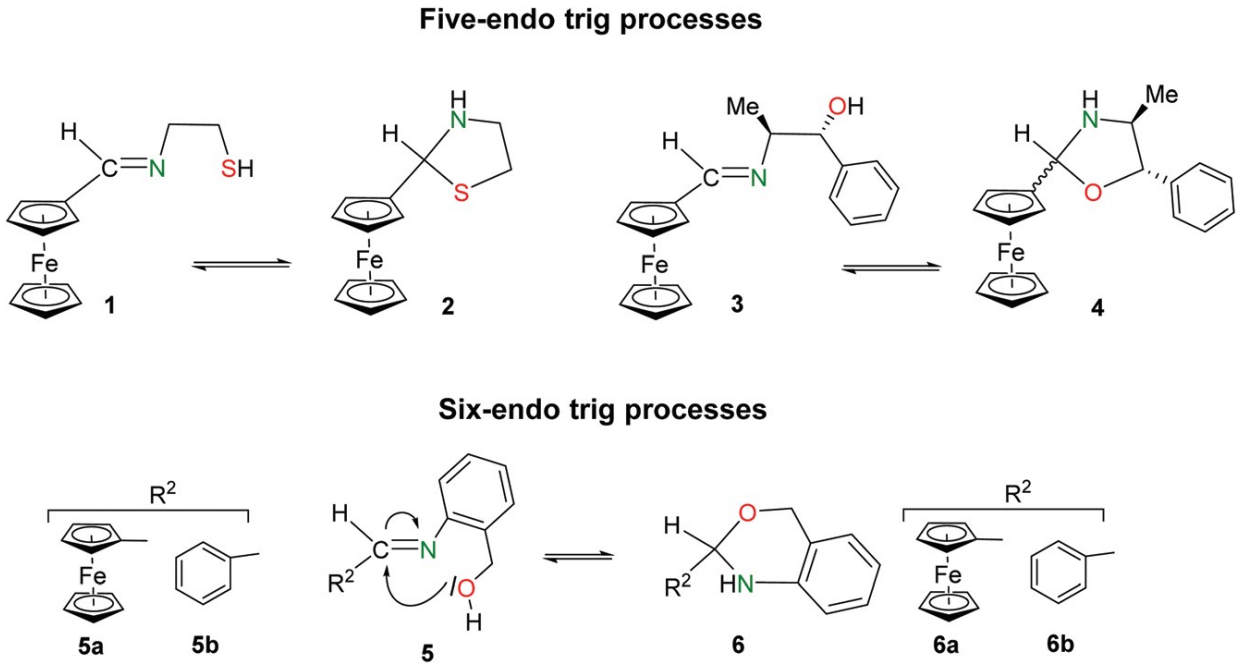
Five-endo trig processes
Six-endo trig processes
1
2
3
4
5
6
5a
5b
6a
6b

SCHEME 2

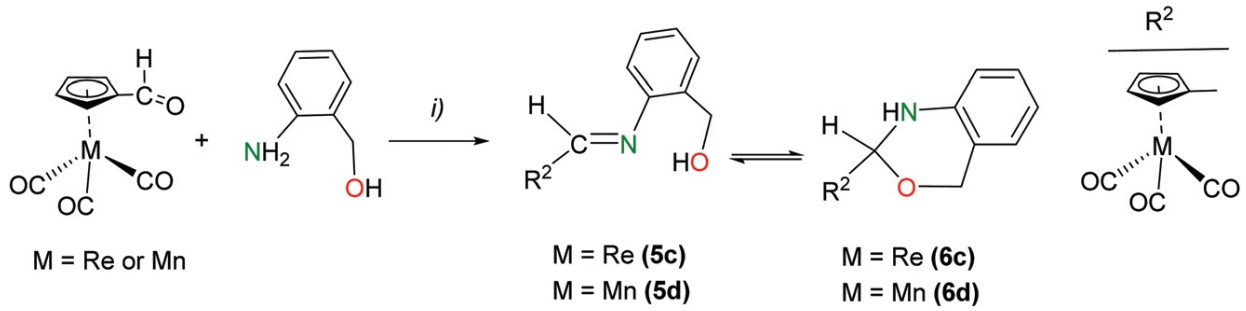

M = Re or Mn

M = Re **(5c)**
M = Mn **(5d)**

M = Re **(6c)**
M = Mn **(6d)**

985 **FIGURE** 3

986

987

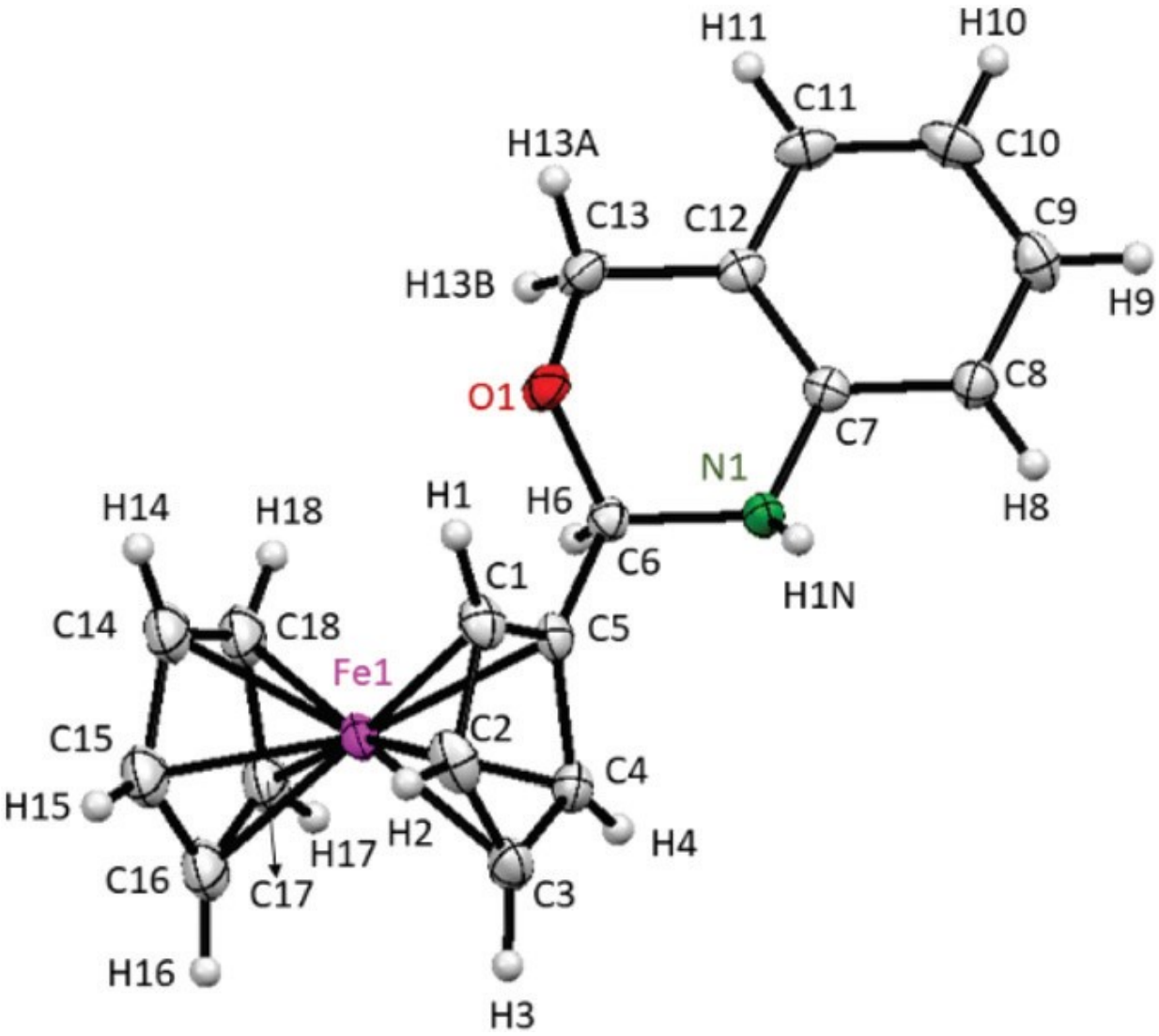

988

989

FIGURE 4

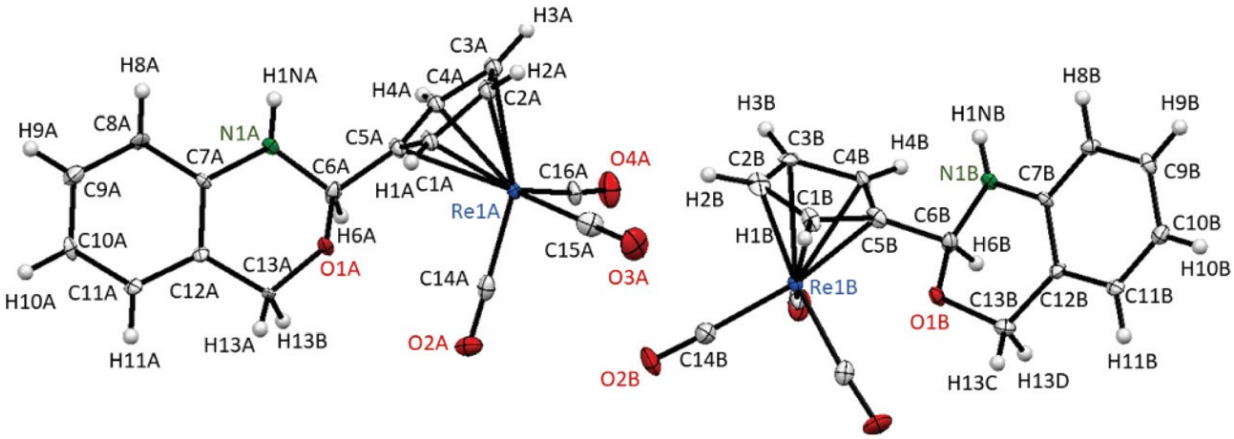
H3A
C3A
H8A
H1NA
C4A
H2A
H4A
C2A
H9A
C8A
N1A
C5A
C7A
C6A
H1A
C1A
C16A
O4A
C9A
Re1A
H6A
C10A
C13A
O1A
C15A
O3A
C14A
H10A
C11A
C12A
H13A
H13B
O2A
H11A
H8B
H9B
H3B
H1NB
C3B
C2B
C4B
H4B
N1B
C7B
C9B
H2B
C1B
C10B
H1B
C6B
C5B
H6B
H10B
Re1B
C13B
C12B
C11B
O1B
O2B
C14B
H13C
H13D
H11B

FIGURE 5

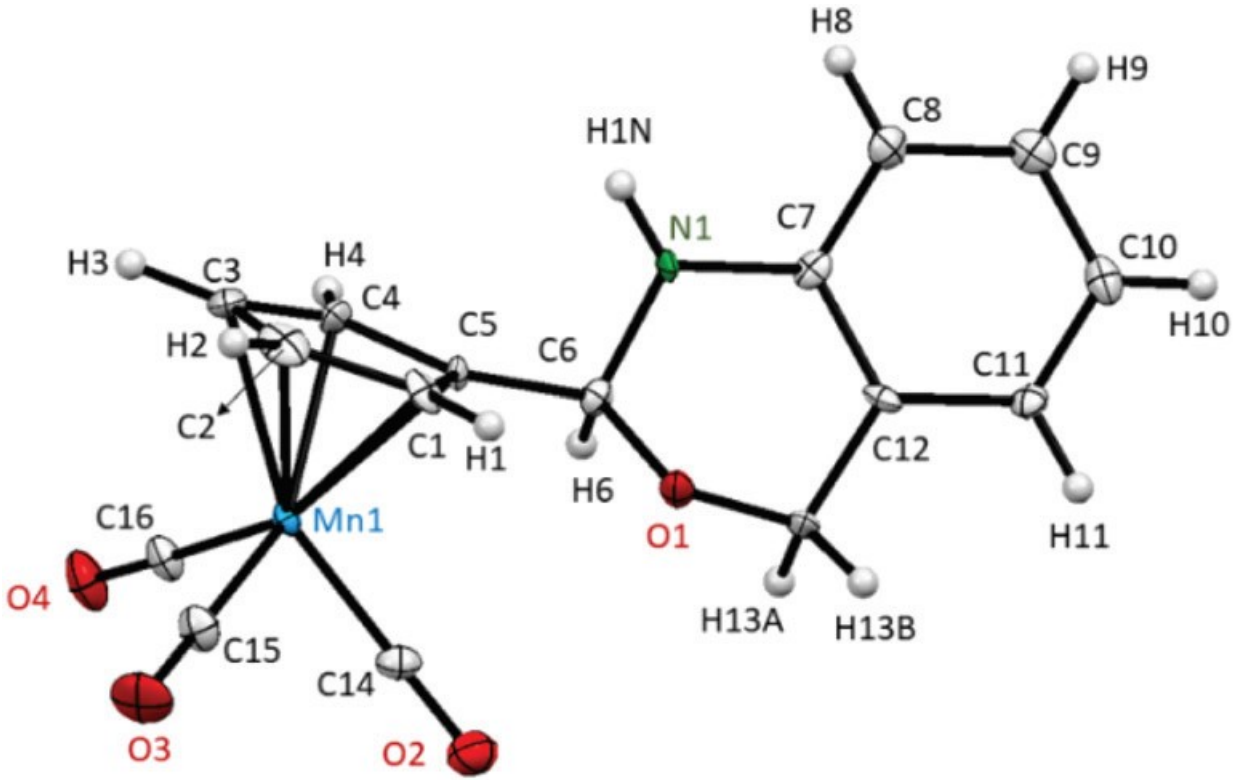
H8
H9
C8
H1N
C9
N1
C7
C10
H3
C3
H4
C4
H10
C5
H2
C6
C11
C2
C1
H1
C12
H6
O1
C16
Mn1
H11
O4
H13A
H13B
C15
C14
O3
O2

FIGURE 6

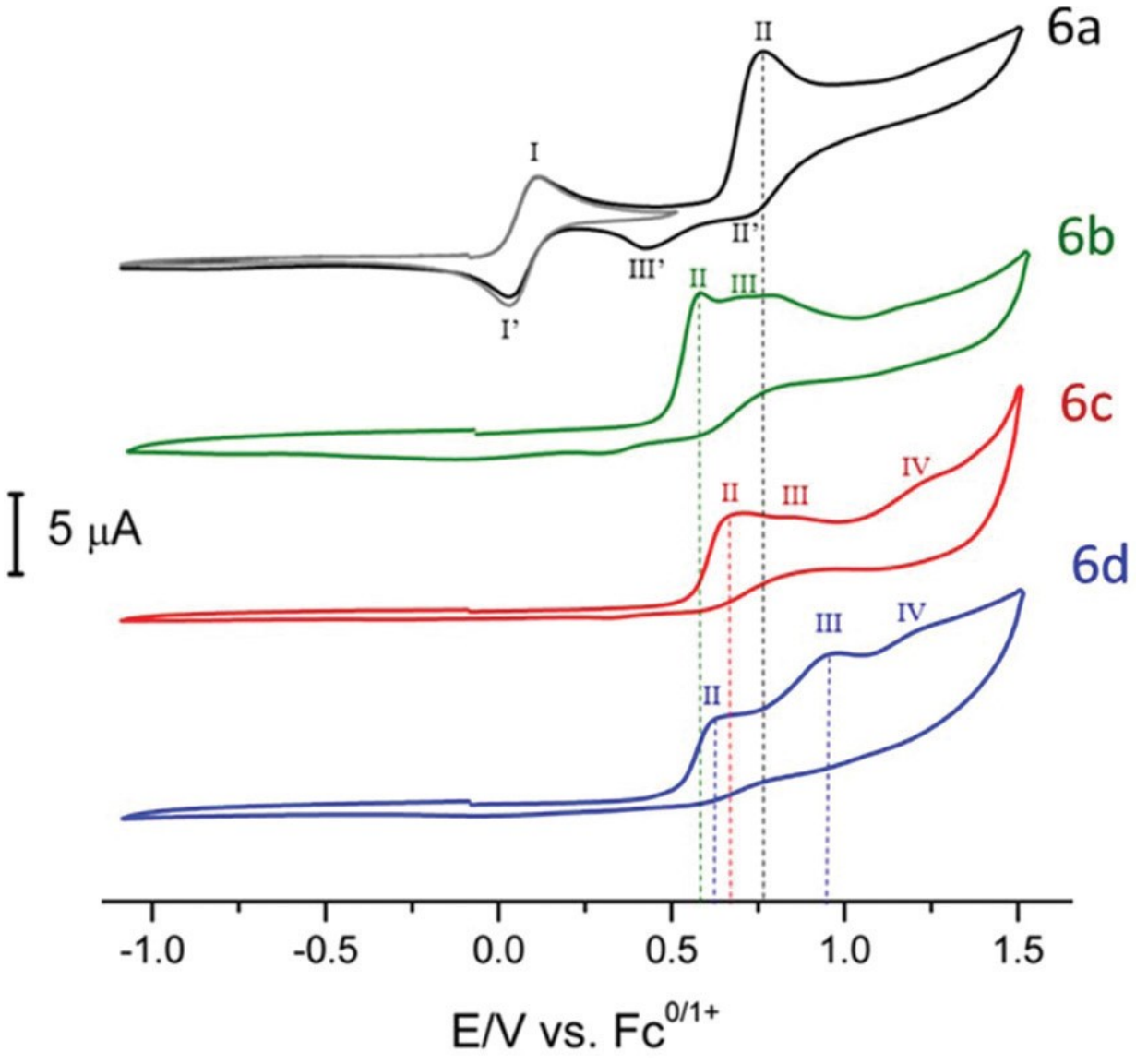
6a
II
I
II'
III'
I'
6b
II
III
6c
IV
II
III
5 μA
6d
III
IV
II
-1.0
-0.5
0.0
0.5
1.0
1.5
E/V vs. Fc0/1+

FIGURE 7

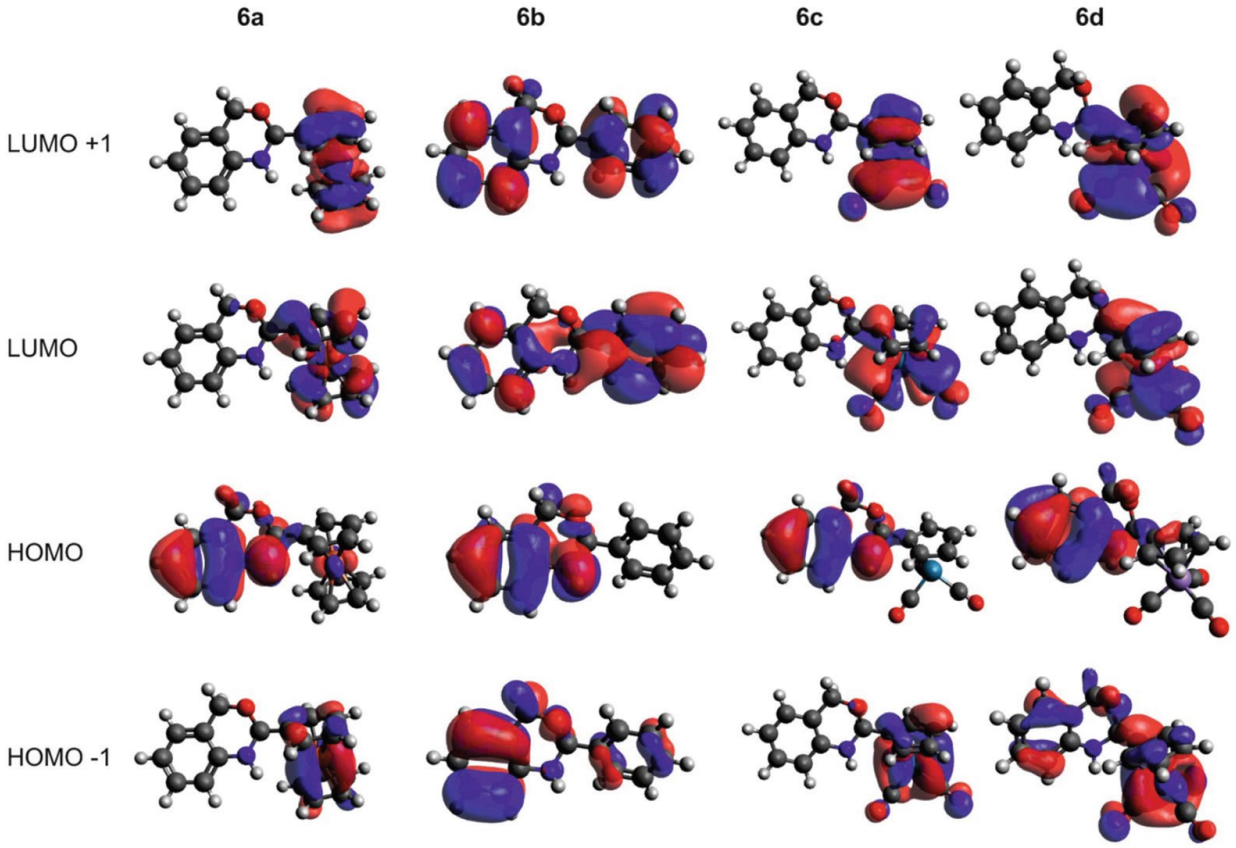

FIGURE 8

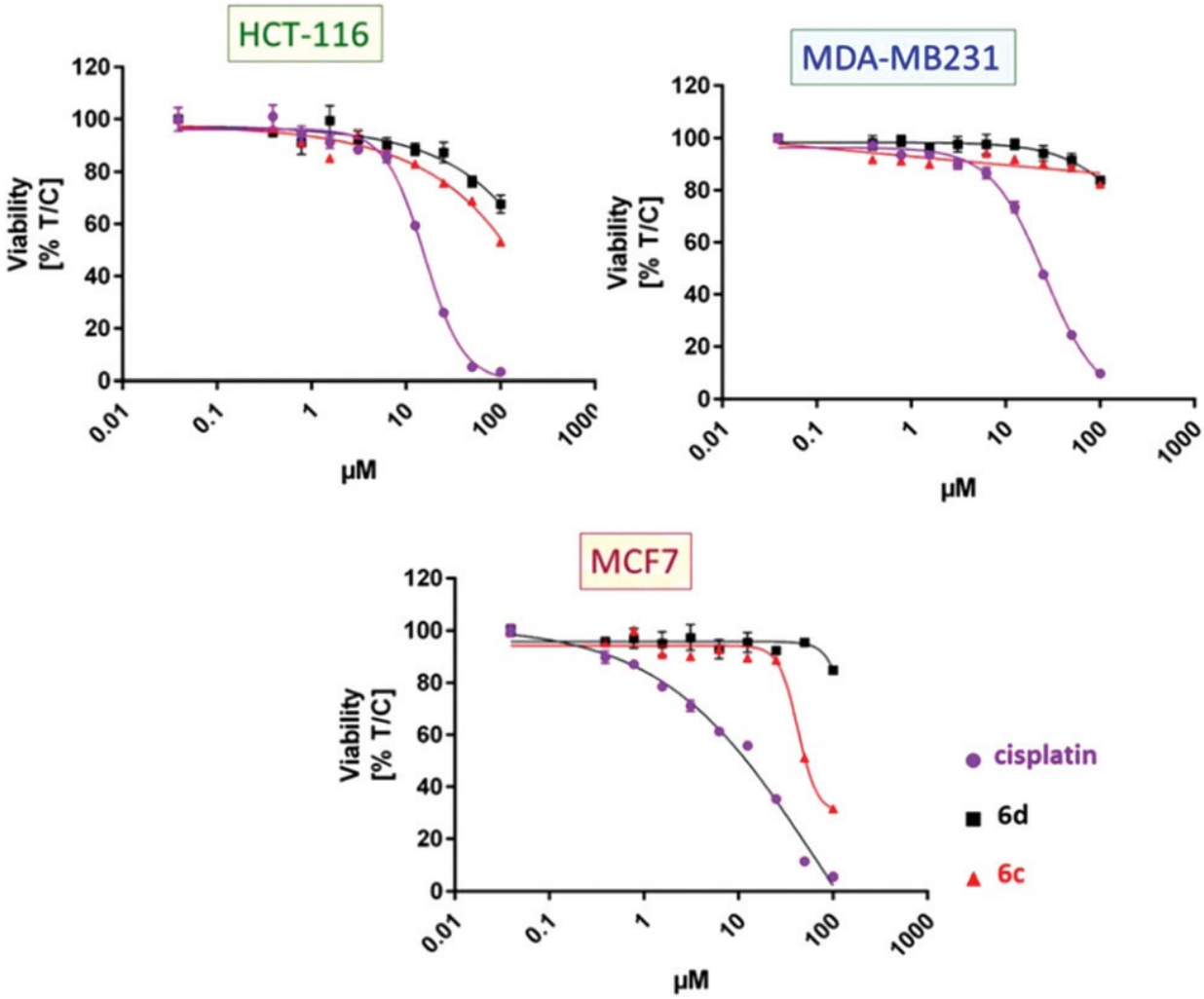
HCT-116
MDA-MB231
MCF7
Viability [% T/C]
120
100
80
60
40
20
0
0.01
0.1
1
10
100
1000
µM
cisplatin
6d
6c

FIGURE 9

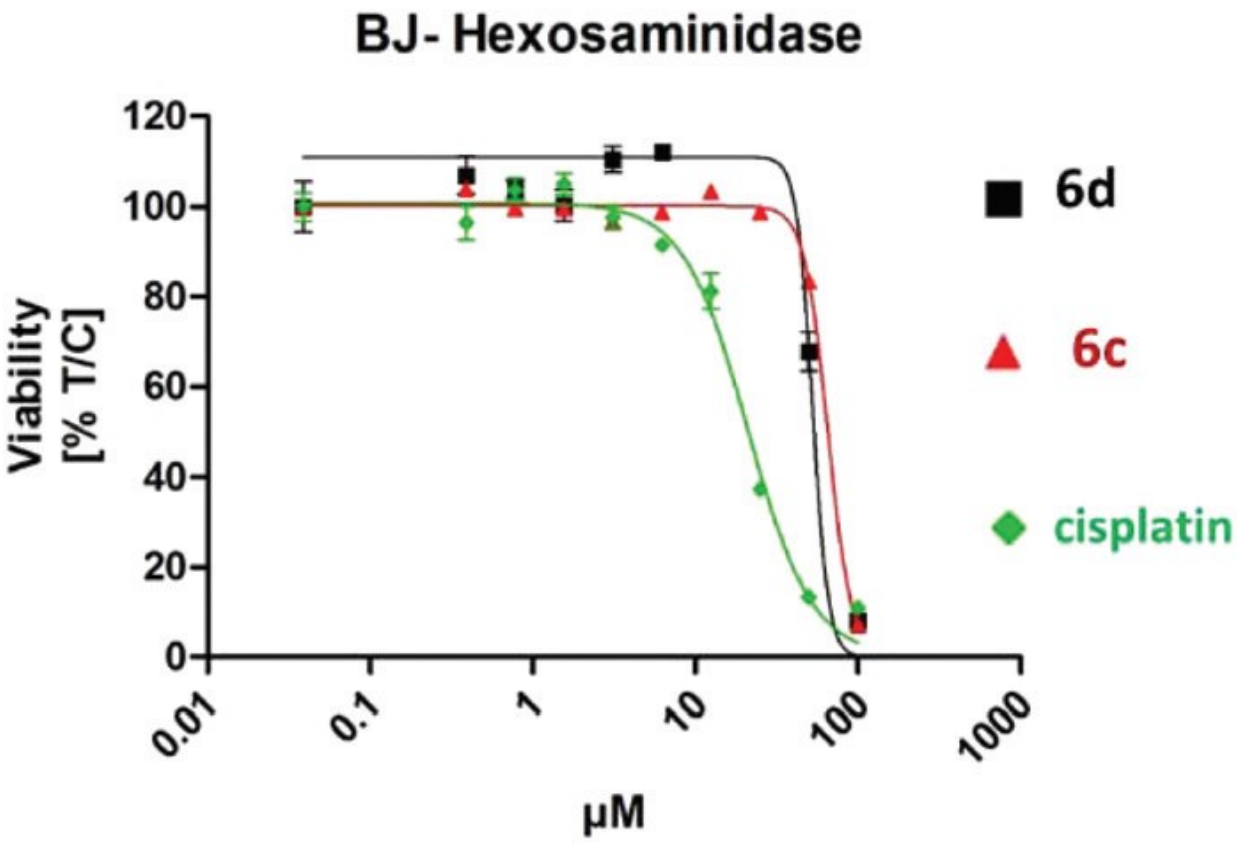
BJ- Hexosaminidase
Viability
[% T/C]
120
100
80
60
40
20
0
0.01
0.1
1
10
100
1000
µM
6d
6c
cisplatin

FIGURE 10

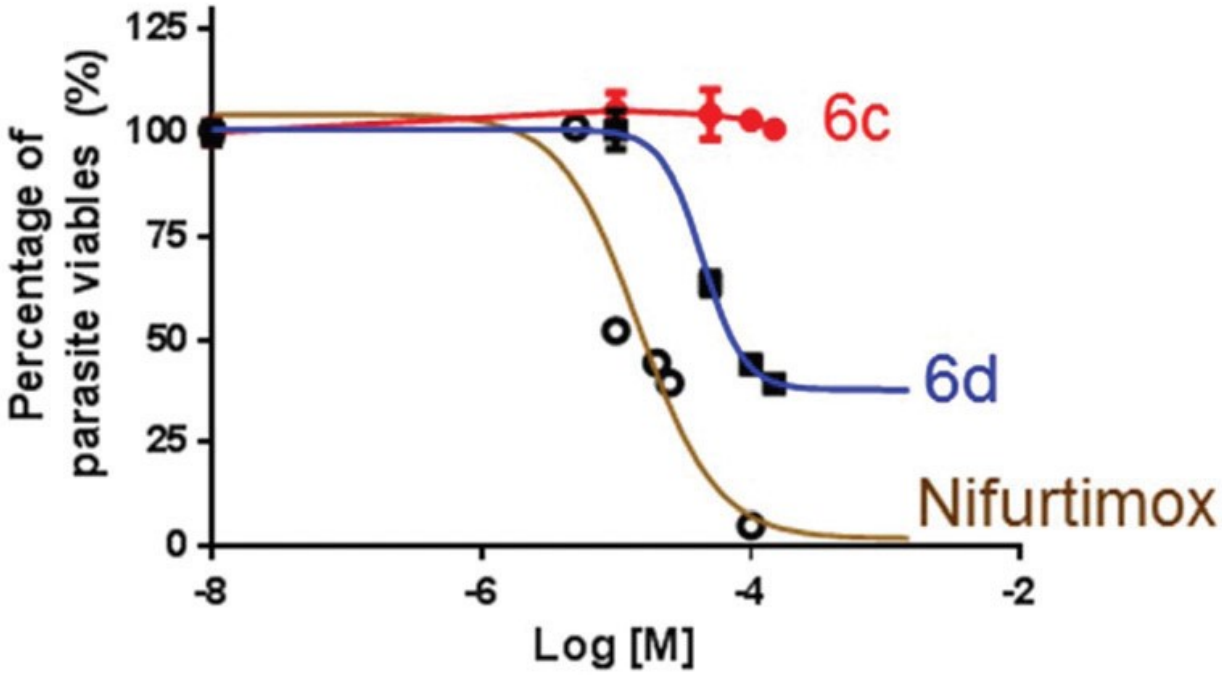
Percentage of parasite viables (%)
125
100
75
50
25
0
-8
-6
-4
-2
Log [M]
6c
6d
Nifurtimox

Table 1 Selected bond lengths (in Å), bond angles (in °) of the 2-ferrocenyl-2,4-dihydro-1H-3,1-benzoxazine (6a) and its analogues with the cyrhetrenyl (in 6c) or the cymantrenyl (in 6d) unit on position 2. Standard deviation parameters are given in parenthesis (see text)

		6c [a]		
	6a	Molecule A	Molecule B	6d
Bond lengths				
O1–C6	1.426(3)	1.420(8)	1.418(8)	1.434(3)
O1–C13	1.431(3)	1.434(9)	1.427(9)	1.421(3)
C6–N1	1.443(3)	1.456(9)	1.444(9)	1.442(3)
N1–C7	1.404(3)	1.415(9)	1.413(9)	1.403(3)
C6–C5	1.494(4)	1.506(10)	1.510(10)	1.494(3)
C7–C8	1.398(3)	1.410(9)	1.383(9)	1.395(4)
C8–C9	1.380(4)	1.390(11)	1.387(9)	1.390(4)
C9–C10	1.389(4)	1.389(10)	1.392(10)	1.401(4)
C10–C11	1.379(4)	1.383(10)	1.373(14)	1.391(4)
C11–C12	1.400(4)	1.395(10)	1.391(10)	1.406(4)
C12–C7	1.395(3)	1.396(9)	1.400(9)	1.400(4)
C12–C13	1.500(4)	1.494(10)	1.511(10)	1.490(3)
$M–C_{(Cp)}$ [b,c]	2.040(3)	2.304(4)	2.302(7)	2.145(6)
$M–C_{(CO)}$ [b]	—	1.920(9)	1.918(6)	1.798(4)
C–C [b,c]	1.42(4)	1.424(15)	1.412(9)	1.433(4)
C–O [b]	—	1.141(14)	1.141(10)	1.155(4)
Bond angles				
O1–C6–N1	111.8(2)	111.9(6)	114.3(6)	111.4(2)
C6–N1–C7	116.2(2)	115.6(6)	114.1(10)	116.8(4)
N1–C7–C12	119.7(2)	119.8(6)	121.3(6)	118.9(2)
C7–C12–C11	118.7(2)	118.3(6)	119.8(7)	118.4(2)
C7–C12–C13	120.0(2)	119.5(6)	118.5(6)	119.5(2)
C11–C12–C13	121.3(2)	121.1(6)	118.5(6)	121.9(2)
C12–C13–O1	112.1(2)	111.8(5)	111.2(5)	112.0(2)
N1–C6–C5	110.3(3)	108.4(6)	109.5(6)	109.8(2)
O1–C6–C5	108.7(2)	108.1(6)	106.6(6)	107.9(2)

[a] Two non-equivalent molecules (A and B) were present in the crystal (see Fig. 4). [b] Average values. [c] In 6a the carbon atoms of non-substituted ring were found in disordered positions, and in this case the Fe–C value given corresponds to the average of the distances between the Fe(II) atom and the carbon atoms of the (C1–C5) ring.

Table 2 Summary of the electrochemical data [anodic (EIpa) potentials and cathodic potential (EI' pc) (in V)]. Data were obtained at a scan rate υ =250 mV s−1 and referenced to the ferrocene/ferricinium (Fc/Fc+) couple. For the identification of the peaks (see also Fig. 6)

Compound	E^{I}_{pa}	E^{II}_{pa}	E^{III}_{pa}	E^{IV}_{pa}	E^{I}_{pc}
6a[a]	0.107	0.751	—	—	0.032
6b	—	0.550	0.799[b]	—	—
6c	—	0.702	0.856[b]	1.235[c]	—
6d	—	0.615	0.942	1.214[c]	—

[a] $\Delta E = E^{I}_{pa} - E^{I}_{pc} = 0.075$ V. [b] For **6b** and **6c** the oxidation peak III was broader and exhibited lower resolution than II (Fig. 6). [c] This peak is attributed to an oxidation process involving the Re(I) atom of **6c** or the Mn(I) in **6d**.

Table 3 Anticancer and antichagasic activities of the new 2-cyrhetrenyl-(6c) or cymantrenyl- (6d) 2,4-dihydro-1H-3,1-benzoxazines (6c and 6d, respectively) (IC50 values in μM)a against: the colon cell line HCT-116, the two breast cancer cell lines [MDA-MB231 and MCF7] and Trypanosoma cruzi epimastigotes (Dm28c strain). For comparison purposes, data obtained for cisplatin in the cancer cell lines or for nifurtimox in Trypanosoma cruzi epimastigotes (Dm28c strain) under identical experimental conditions are also included

	Anticancer activity			Anti-*Trypanosoma Cruzi* activity
	IC_{50} values in the cancer cell lines			IC_{50} values in epimastigotes
Compound	HCT-116	MDA-MB231	MCF7	(Dm28c strain)
6c	>100	>100	51 ± 4	[b]
6d	>100	>100	>100	43.4 ± 0.9
Cisplatin	16 ± 2	26 ± 3	13 ± 4	—
Nifurtimox	—	—	—	17.4 ± 0.3

[a] Data are shown as the mean values of two experiments performed in triplicate with the corresponding standard deviations. [b] Inactive (see also Fig. 10).